

STRUCTURAL AND FUNCTIONAL
CEREBELLAR NETWORKS
IN THEORY OF MIND

A Dissertation
Submitted to
the Temple University Graduate Board

In Partial Fulfillment
of the Requirements for the Degree
DOCTOR OF PHILOSOPHY

by
Athanasia Metoki
December 2020

Examining Committee Members:

Ingrid Olson, Advisory Chair, Department of Psychology
Jason Chein, Department of Psychology
Vishnu Murty, Department of Psychology
Geoffrey Wright, Departments of Physical Therapy and Bioengineering, College of Public Health
Huilin Peng, Department of Psychology
Nico Dosenbach, External Member, Washington University in St. Louis

ABSTRACT

Theory of Mind (ToM) is the ability to infer mental states of others and this skill relies on a distributed network of brain regions. A brain region that has been traditionally disregarded in relation to non-motor functions is the cerebellum. Here, we leveraged large-scale multimodal neuroimaging data to elucidate the structural and functional role of the cerebellum in ToM. We used functional activations to determine whether the cerebellum has a domain-general or domain-specific functional role. We found that the cerebellum is organized in a domain-specific way. We used effective connectivity and probabilistic tractography to map the cerebello-cerebral ToM network. We found a left cerebellar effective and structural lateralization, with more and stronger effective connections from the left cerebellar hemisphere to the contralateral cerebral ToM areas and greater cerebello-thalamo-cortical (CTC) and cortico-ponto-cerebellar (CPC) streamline counts from and to the left cerebellum. Lastly, we examined the relationship between CTC and CPC white matter and ToM speed and accuracy but found no correlation. Our study provides novel insights to the network organization of the cerebellum, an overlooked brain structure, and ToM, one of humans' most essential abilities to navigate the social world.

This dissertation is dedicated
to everyone who never
had a doubt.

ACKNOWLEDGMENTS

Throughout the writing of this dissertation, I have received a great deal of support and assistance.

I would like to thank my mentor Dr. Ingrid Olson. She was a wonderful mentor, helpful and supportive, allowing me to grow with steady guidance. She has been an invaluable ally during the five years of my graduate work.

I would also like to thank the members of my doctoral committee: Dr. Jason Chein, Dr. Vishnu Murty, Dr. Geoffrey Wright, Dr. Huiling Peng, and Dr. Nico Dosenbach. Their suggestions and feedback had a great impact to this dissertation.

I would like to acknowledge my labmates from the Olson lab for their wonderful collaboration. Thank you Kylie Alm, Zoe Ngo, Tehila Nugiel, Linda Hoffman, Susan Benear, Haroon Popal and everyone else in the lab. Our conversations over the years shaped this dissertation. I would particularly like to single out Dr. Yin Wang. This dissertation, and my PhD as a whole, would have been very different if it hadn't been for our collaboration, your help and our stimulating discussions. Thank you.

In addition, I would like to thank my family and friends. My sister, my brother, my grandmother, great-aunts and great-uncle, my aunt and cousins, my best friend, and my father. More importantly, I want to thank my mother and my grandfather. If it hadn't been for your support, trust in me, and financial assistance I would still be a social worker in Asprovalta. I owe you everything because you made this happen.

Last but certainly not least, I want to thank my husband Dr. Aris Sotiras and my son Yanni. Without my husband's support and "destructive criticism" I may have been

writing acknowledgements for a completely different dissertation. Without Yanni in my life I wouldn't have known that it is possible to run analyses and write a dissertation while taking care of a baby. It is extremely hard, I wouldn't recommend it to anyone, but it is possible. I love you both immensely and you are my world. Thank you.

TABLE OF CONTENTS

	Page
ABSTRACT.....	ii
DEDICATION.....	iii
ACKNOWLEDGMENTS	iv
LIST OF TABLES.....	viii
LIST OF FIGURES	ix
CHAPTER	
1. INTRODUCTION	1
Social Cognition and Theory of Mind	1
The Cerebellum.....	2
The Current Study.....	8
2. METHODS	9
Dataset and Participants.....	9
Overview of HCP protocol	9
In-scanner Tasks	10
Social Cognition (Theory of Mind)	11
Motor.....	11
Gambling.....	12
Working Memory.....	13
Language Processing	13
Relational Processing.....	13

Emotion Processing	14
Image Preprocessing	15
Regions of Interest Definition.....	15
Cluster Overlap and Euclidean Distances.....	18
Psychophysiological Interaction Analyses	19
Diffusion Analyses.....	21
Brain-behavior Association	22
3. RESULTS	23
Testing Hypothesis 1: Functions of Distinct Cerebellar Regions.....	23
Testing Hypothesis 2: Effective Connectivity between ToM Cerebellum and Cerebrum.....	27
Testing Hypothesis 3: Structural Connectivity between ToM Cerebellum and Cerebrum.....	32
Testing Hypothesis 4: Brain-behavior Association	35
4. DISCUSSION	37
Limitations and Future Directions	42
Conclusions.....	43
REFERENCES CITED.....	44
APPENDIX	
SUPPLEMENTARY TABLES	74

LIST OF TABLES

Table	Page
1. Activation clusters and cerebellar lobe percent overlap.....	25
2. Percentage of overlap between activation clusters.....	26
3. Mean cerebello-thalamo-cortical (CTC) and cortico-ponto-cerebellar (CPC) streamline counts.....	34
A1. Cerebellar clusters of activation and cerebellar lobule percentage overlap.....	74
A2. One-sample Kolmogorov-Smirnov test for normality distribution of beta weights (effective connectivity) of all tasks.....	74
A3. Spearman’s rho correlations between task activations.....	75
A4. Wilcoxon signed-rank test results for all possible task pairs.....	75
A5. Paired samples t-tests on individual beta-weights (effective connectivity) for all proximal ROIs.....	76
A6. Wilcoxon signed ranks test on individual beta-weights (effective connectivity) for proximal ROIs not meeting normality criteria.....	77
A7. Cerebello-thalamo-cortical white matter pathways average streamline counts...	78
A8. Cortico-ponto-cerebellar white matter pathways average streamline counts.....	80
A9. One-sample Kolmogorov-Smirnov test for normality distribution of cerebello-thalamo-cortical and cortico-ponto-cerebellar white matter pathway streamline counts (cerebellar lobe averages).....	82
A10. Spearman’s rho correlations between cerebello-thalamo-cortical streamline counts averaged across cerebellar lobes.....	83
A11. Spearman’s rho correlations between cortico-ponto-cerebellar streamline counts averaged across cerebellar lobes.....	84
A12. Wilcoxon signed-rank test results for all possible left-right streamline count cerebellar hemisphere and lobe pairs.....	85

LIST OF FIGURES

Figure	Page
1. Social cognition (Theory of Mind) task.....	12
2. Group-level task clusters of activation.....	23
3. Local maxima for each functional task.....	24
4. Data-driven cerebellar ToM local maxima.....	28
5. Effective connectivity between cerebellar and cerebral ToM ROIs.....	30
6. Effective connectivity significance between cerebellar and cerebral ToM ROIs.....	31
7. Mean streamline counts for each cerebello-thalamo-cortical and cortico-ponto- cerebellar white matter tract.....	33

CHAPTER 1

INTRODUCTION

Social Cognition and Theory of Mind

Social cognition broadly encompasses the cognitive processes that humans use to navigate the social world (Amodio & Frith, 2006; Beer & Ochsner, 2006; Frith & Frith, 2007, 2012; Van Overwalle, 2009; Van Overwalle & Baetens, 2009). Through verbal and non-verbal input humans manage to detect intentionality, make informed judgements, attribute emotions and successfully navigate the world. A lack of social cognitive skills could lead to misjudgment of social situations and interactions with other people, making every-day life an extremely difficult experience.

Attributing mental states to others, and interpreting their intentions, perspectives, and beliefs is termed mentalizing or Theory of Mind (ToM) (Blakemore, 2008; Frith & Frith, 2006; Mar, 2011; Schurz et al., 2014) and is an essential social skill. An extensive literature in social neuroscience has identified brain areas that work in concert subserving this process. These collective brain areas form a large-scale neural network: the mentalizing network. The mentalizing network comprises the occipital gyrus, fusiform gyrus, temporoparietal junction, precuneus, amygdala, anterior temporal lobe, inferior frontal gyrus, and medial prefrontal cortex (which can be further divided to dorsomedial and ventromedial prefrontal cortex) (Bzdok et al., 2013, 2015; Hartwright et al., 2016; Lahnakoski et al., 2012; Uddin et al., 2007; Yang et al., 2015). Although there is a rich body of neuroimaging studies that examines these social brain areas, their function, and their connectivity, there is one brain structure that has been systematically overlooked by social neuroscientists: the cerebellum.

The Cerebellum

The cerebellum is located below the occipital lobes, posterior to the pons and medulla oblongata. Traditionally the cerebellum has been considered a motor brain area. Starting with the work of Jean Marie Pierre Flourens (1842), who demonstrated that cerebellar damage in pigeons resulted in impaired flight due to loss of coordination of voluntary wing movements, and following with studies in monkeys (Luciani, 1892; Ferrier and Turner, 1894; Russell, 1894), and observations by pioneering clinical neuroscientists (Sanger Brown, 1892; Pierre Marie, 1893; Felix Babinski, 1899; Holmes, 1908, 1917, 1939), the notion that the cerebellum is engaged solely in motor functions, was a view that solidified as a well-known absolute truth over the decades. What was overlooked though was that evidence of intellectual and emotional disability in patients with cerebellar damage or agenesis was also reported (Fisher, 1839; Zanatta, 2018). The disregard, or sometimes aversion, towards mental health issues in the late 19th century led to refusal to consider a cerebellar role beyond the coordination of voluntary motor activity for almost 200 years.

In more recent years there has been a newfound interest in the cerebellum and its non-motor functions. Although the majority of the cerebellum-related research is still centered around motor related actions, such as the coordination of voluntary movements, gait, posture, and speech (Brodal & Bjaalie, 1997; Fine et al., 2002; Glickstein, 1992, 1993; Ito, 2002), researchers have started shifting their attention on its non-motor role, contemplating new theories of cerebellar function (Leiner et al., 1986; Schmahmann, 1991, 1998), and investigating its anatomical properties (Middleton & Strick, 1994; Schmahmann & Pandya, 1989, 1997). These investigations were prompted by anatomical

tracer studies in animals which showed that cerebello-cerebral structural connectivity was different between primates and other vertebrates, with primate cerebellar output fibers reaching the frontal association cortex (Ito, 1984). Additional primate studies using viral retrograde transneuronal tracing methods showed not only that the cerebellum projects to specific premotor and prefrontal cortex (Brodmann areas 9 and 46 which correspond to the dorsolateral/medial prefrontal cortex) (Clower et al., 2005; Dum & Strick, 2003; Kelly & Strick, 2003) but also that these cortical areas project back to specific cerebellar areas forming closed cerebro-cerebellar loops (Middleton & Strick, 1997, 2001; Schmahmann & Pandya, 1997).

Post-mortem studies in the human brain also showed that while the phylogenetically older anterior portion of the cerebellum has connections to motor cortex, the phylogenetically newer posterior cerebellar lobe projects to the frontal lobe (Leiner et al., 1993). The functional significance of these connections was illuminated by work showing that cerebellar damage could at times cause the “Cerebellar Cognitive Affective Syndrome” which includes personality changes, blunting of affect, disinhibition or inappropriate behavior, as well as language deficits such as mutism, dysprosodia, and anagrammatism (Schmahmann & Sherman, 1998).

Subsequently, a number of studies, using neuroimaging methods (e.g. Positron Emission Tomography (PET) or functional magnetic resonance imaging (fMRI)) reported cerebellar activations to various linguistic tasks (Petersen et al., 1988, 1989), specifically in lobule VI and Crus I (Ackermann et al., 1998; Desmond et al., 1997; Fiez & Raichle, 1997; Martin et al., 1995; Raichle et al., 1994). Consistent with the crossed cerebro-cerebellar fiber pathways, linguistic impairments can arise following right cerebellar

hemisphere lesions, whereas visual–spatial difficulties may follow left cerebellar hemisphere damage (Fiez et al., 1992; Gottwald et al., 2004; Gross-Tsur et al., 2006; Hokkanen et al., 2006; Riva & Giorgi, 2000; Scott et al., 2007). Other studies reported that different cerebellar regions, lobules VIIb, VIIIa, and Crus I, are active during various working memory tasks, a finding replicated multiple times (Ravizza et al., 2006; Schmahmann & Sherman, 1998; Silveri et al., 1998). Several studies have also shown activation in the cerebellar vermis during behaviors related to emotions (Lane et al., 1997; Reiman et al., 1989, 1997) and affective processing.

From a clinical perspective, cerebellar, social cognition, and emotion processing impairments have been observed in multiple neuropsychiatric and neurodevelopmental disorders, including attention-deficit/hyperactivity disorder (ADHD) (Mackie et al., 2007), autism spectrum disorder (ASD; Bailey et al., 1998; Catani et al., 2008; Palmen et al., 2004; Whitney et al., 2008), major depressive disorder (Shah et al., 1992), and schizophrenia (Segarra et al., 2008). Children with ASD, that presented with constrictions in social interaction, had hypoplasia in the cerebellar vermis lobules VI and VII compared to healthy controls (Courchesne et al., 1994), although other studies have found evidence of cerebellar vermis hyperplasia (Courchesne et al., 1994). In a diffusion tensor imaging study, Catani et al. (2008) demonstrated that individuals with Asperger syndrome had reduced axonal density in short fibers in the right cerebellar peduncle while no differences were observed in the afferent fiber density. Furthermore, it has been suggested that cerebellar alterations interrupt functional connectivity with the cerebral cortex, which results in decreased release of dopamine in the frontal cortex (Mittleman et al., 2008). Multiple neuroimaging studies also propose that cerebellar abnormalities are

observed in individuals with schizophrenia. Cerebellar grey and white matter volume reductions have been reported (Segarra et al., 2008; Sharma et al., 1998), including vermal volume reduction (Heath et al., 1982; Jacobsen et al., 1997; Lippmann et al., 1982; Varnäs et al., 2007). Lastly, a reduced vermis volume has been found in individuals with bipolar disorder (Delbello et al., 1999) and major depressive disorder (Shah et al., 1992).

It is clear that the cerebellum plays a role not only in motor functions but in non-motor as well, including social cognition. But what is the exact role of the cerebellum in all these functions? In the motor literature there is agreement that the cerebellum contributes in the regulation of the rhythm, rate, accuracy, and force of movements (for a review see Manto et al., 2012). Similarly, it is considered that the cerebellum regulates the capacity, speed, appropriateness and consistency of mental processes. The theory that the cerebellum maintains behavior around a homeostatic baseline is termed the “dysmetria of thought theory” (Schmahmann, 1998) and it is analogous to the dysmetria of movement theory. The latter is presented with overshooting and lack of control in the motor system. In the dysmetria of thought theory, these are equated with unpredictability in social interactions, a mismatch between reality and perceived reality, and unsuccessful, illogical efforts to correct errors in behavior and thought (Schmahmann, 2019). It is clear that dysmetria of movement is matched with dysmetria of thought and this match in functions is explained by the theory of the Universal Cerebellar Transform (UCT; Schmahmann, 2000, 2001, 2004) according to which there is a unique computation to the cerebellum applying to all functions (movement- and cognition-related) due to the uniform cortical cytoarchitectonic organization of the cerebellum (Ito, 1993; Voogd &

Glickstein, 1998) which is applied to all its functions (Guell, Gabrieli, et al., 2018; Schmahmann, 2000, 2001, 2004). The most prominent theory about the nature of the cerebellar computation posits that the cerebellum is encoding internal models that reproduce the dynamic properties of body parts for controlling these body parts without any sensory feedback, and for mental processes, that it encodes internal models which reproduce the essential properties of mental representations in the cerebral cortex (Ito, 2008).

So how can we best define and explore the role of the cerebellum in social cognition, anatomically and functionally? Van Overwalle and colleagues proposed and showed through meta-analyses that the cerebellum is specifically involved in ToM and somatomotor processes (Van Overwalle, Baetens, et al., 2015; Van Overwalle, D’aes, et al., 2015; Van Overwalle & Mariën, 2016). This idea drew heavily on findings by (Buckner et al., 2011) showing at the group level that the cerebellum is linked to the default network, which in turn has been linked to ToM, with a triple representation of cognitive domains in the cerebellar posterior lobe, specifically lobules VI-Crus I, Crus II-VIIb, and lobule IX. In a recent study, Guell, Gabrieli, et al. (2018) confirmed and extended Buckner’s demonstration using the Human Connectome Project dataset (Van Essen et al., 2013). Consistent with this, (Hoche et al., 2016) found that patients with cerebellar damage are impaired in a task of emotion attribution from faces, supporting the notion of the importance of the cerebellum in social cognition.

Regarding anatomical connectivity, few studies have employed diffusion-weighted imaging techniques and tractography to confirm in-vivo the existence of white matter connections in humans between the cerebellum and the cerebral cortex and

explore their quality. Salamon et al. (2007) were able to delineate the cerebellar peduncles using diffusion tensor imaging (DTI). Jissendi et al. (2008) were the first to isolate cerebellar projections to prefrontal and posterior parietal cortices using tractography. They were the first to show these pathways in humans in-vivo even though they were not able to extract pathways for all 10 of their subjects and their DTI protocol was rudimentary but reasonable for the year the study was conducted. Salmi et al. (2010) used task-fMRI and diffusion-weighted MRI with probabilistic tractography with a nonverbal auditory working memory task and found that cognitive and motor functions are segregated in the cerebellum. They did not delineate the whole cerebro-cerebellar loop, but fragments of the loop interconnecting at the pons and the thalamus. Granziera et al. (2009) conducted a diffusion spectrum imaging study identifying several white matter connections in four subjects. The white matter connections they traced were predominately within the cerebellum (i.e. deep cerebellar nuclei to cerebellar cortex) or up to the pons and thalamus, but not all the way to the cerebral cortex. Sokolov et al., (2014) were the first group that delineated the cerebro-cerebellar white matter loop from the right posterior superior temporal sulcus to the left cerebellar lobule Crus I. Keser et al. (2015) was the first group to explore the full extent of the white matter feedforward and feedback pathways between the cerebellum and the cerebral cortex. They used deterministic tractography to reconstruct the spinocerebellar pathway, the dentate-rubro-thalamo-cortical pathway (feedforward, cerebellar origin), and the cortico-ponto-cerebellar pathways (feedback, cerebral cortex origin) which comprise of the fronto-ponto-cerebellar, parieto-ponto-cerebellar, temporo-ponto-cerebellar and occipito-ponto-cerebellar pathways. This study's findings were important because they clearly

demonstrated that the white matter connections between the cerebellum and cerebral cortex are diverse, both contralateral and ipsilateral, and not solely involving the motor cortex. Yet the study had some limitations such as the use of deterministic tractography instead of probabilistic (Behrens et al., 2007), the small number of participants (n=10), and the fact that their results would not survive multiple comparisons due to the small sample size (Keser et al., 2015). Furthermore, the researchers did not demonstrate lobular variation in the dentate-rubro-thalamo-cortical pathway. Karavasilis et al. (2019) confirmed the results by Keser et al. (2015) by replicating their study with a larger number of participants (n=60).

The Current Study

Proof of functional connectivity and anatomical connectivity between the cerebellum and the cerebral cortex is evident. Yet the functional relationship and anatomical connectivity between the ToM areas of the cerebellum and the ToM areas of the cerebral cortex, remains unknown.

The goal of this study is to bring together disparate findings linking ToM processing to portions of the cerebellum by testing the following hypotheses:

1. There are distinct cerebellar regions related to ToM;
2. Portions of the cerebellum functionally interact with portions of the cerebrum to solve social tasks;
3. There are white matter networks linking the cerebellum to cerebral regions involved in ToM;
4. White matter microstructural indices are correlated with behavioral indices of ToM.

CHAPTER 2

METHODS

Dataset and Participants

All data used in this study are part of the Human Connectome Project (HCP) dataset, specifically the WU-Minn HCP Consortium S900 Release (WU - Minn Consortium Human Connectome Project, 2015). This dataset is publicly available, accessible at <https://www.humanconnectome.org>. Only subjects that completed all imaging sessions of interest (T1/T2, task fMRI (tfMRI), and diffusion MRI (dMRI)) were included in this study. To reduce variance in structural organization (McKay et al., 2017) we restricted our population to only right-handed subjects using the Edinburgh Handedness questionnaire (Oldfield, 1971), which resulted in 679 healthy young adults. Additionally, five subjects were excluded due to lack of enough robust signal in all bilateral ROIs in the ToM localizer task, and one more subject for missing all the explanatory variable files with timing information necessary for psychophysiological interaction (PPI) analyses, thus leading to a final sample of 671 healthy young adults (377 females, $M=28.78$, $SD=3.67$). Unless otherwise stated, all significant results reported in this study were corrected for multiple comparisons using the false discovery rate (FDR; Benjamini & Hochberg, 1995).

Overview of HCP protocol

Due to the complexity of the HCP data acquisition and preprocessing pipelines, listing all scanning protocols and data analysis procedures in detail is beyond the scope of this dissertation. Full detailed description of all protocols and procedures can be found elsewhere (Barch et al., 2013; Glasser et al., 2013; S. M. Smith et al., 2013; Van Essen et

al., 2012). Briefly, the HCP protocol includes acquisition of structural MRI (0.7mm isotropic voxels), resting-state fMRI (rfMRI) (2mm isotropic voxels, four runs of 1200 volumes, TR = 720ms, 14m33sec per run), tfMRI (2mm isotropic voxels, TR = 720ms, tasks: working memory, gambling, motor, language processing, relational processing, social cognition, emotion processing), and dMRI (1.25mm isotropic voxels, three shells of $b = 1000, 2000, \text{ and } 3000\text{s/mm}^2$, 90 diffusion-weighting directions acquired with right-to-left and left-to-right phase encoding) in a customized Siemens 3T “Connectome Skyra” scanner, with subsets of the subjects getting further scanning in a 7T scanner and a combined MEG/EEG (resting-state and task-evoked) session. Participants also received extensive behavioral testing (Barch et al., 2013): NIH Toolbox for Assessment of Neurological and Behavioral Function (cognition, emotion, motor, sensory), The University of Pennsylvania Computerized Neuropsychological Testing (personality, psychiatric, and additional cognitive and emotion measures), and the Semi-Structured Assessment for the Genetics of Alcoholism (SSAGA; psychiatric and substance use questionnaires). Additional measures that were obtained included, among others, demographics information, health measures, sleep pattern, drug screening.

In-scanner Tasks

Participants were assessed in seven major domains: 1) social cognition; 2) motor (visual, motion, somatosensory, and motor systems); 3) gambling; 4) working memory/cognitive control systems and category specific representations; 5) language processing (semantic and phonological processing); 6) relational processing; and 7) emotion processing (Barch et al., 2013).

Social Cognition (Theory of Mind)

In the social cognition task (henceforth “ToM”), participants viewed short video clips (20s each) of geometrical shapes (circles, squares, triangles) that either interacted or moved purposelessly on the screen (Figure 1). The videos were developed by either Castelli et al. (2000) or Wheatley et al. (2007) and have been validated as a measure of ToM given evidence that they generate task related activation in brain regions associated with ToM with reliable results across subjects (Barch et al., 2013; Castelli et al., 2000, 2002; Wheatley et al., 2007; White et al., 2011). After each video clip participants were asked to select whether the shapes interacted in a socially meaningful way (e.g. playing, dancing, coaxing) with each other taking into account each other’s feelings or thoughts, whether there was no obvious interaction and the shapes moved randomly, or they could select that they weren’t sure. Each of the task’s two runs had five video blocks, two socially meaningful and three random in one and three socially meaningful and two random in the other, and five fixation blocks.

Motor

The motor task was an adaptation of the task developed by Buckner and colleagues (Buckner et al., 2011; Yeo et al., 2011) and was intended to map the motor areas of the brain. Participants were presented with visual cues that asked them to either tap their right or left fingers, squeeze their right or left toes, or move their tongue. Each block of a movement was preceded by a 3s cue and lasted 12s (10 movements). Each of the two runs, consisted of 13 blocks, with two blocks of tongue movements, four of hand movements (two right and two left), and four of foot movements (two right and two left).

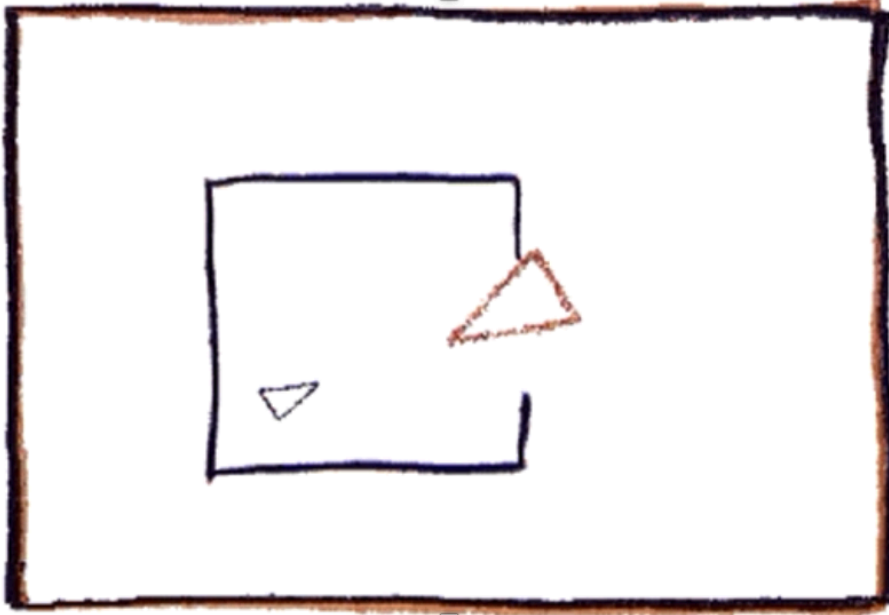


Figure 1. Social cognition (Theory of Mind) task. Snapshot of a video clip from the Theory of Mind task, were two triangles interacted in a socially meaningful way. In this video clip, the triangles were displaying playful behavior with each other, acting as if they were family or close friends. The smaller triangle was excitedly following and nudging the larger one. In other video clips the triangles did not interact at all and were moving in a completely random manner.

Gambling

The gambling task was a modified version of the task developed by Delgado et al. (2000). In this task, participants were presented with a card and they were asked to guess whether the “?” symbol in the card represents a number bigger or smaller than 5. After they guessed they received feedback: The number which was represented by the “?” and a green upward arrow with “\$1” for reward trials, a red downward arrow with “-\$0.50” for loss trials, and the number 5 and a gray double headed arrow for neutral trials. The “?” was presented for 1500ms followed by feedback for 1000ms and a 1000ms intertrial interval with a “+”. The task was presented in blocks of eight trials that were either

mostly reward or mostly loss. In each of the two runs, there were two mostly reward and two mostly loss blocks, interleaved with four fixation blocks (15 seconds each).

Working Memory

In this task participants were presented with blocks of trials consisting of images of faces, places, tools, and body parts. Each run included the four stimulus types presented in separate blocks. Within each run half of the blocks used a 2-back working memory task while half used a 0-back working memory task. Each run contained eight task blocks (10 trials of 2.5s each) and four fixation blocks (15s). On each trial, the stimulus was presented for 2s, followed by a 500ms intertrial interval (ITI).

Language Processing

The language processing task (henceforth “language”) was developed by Binder et al. (2011). The task consisted of two runs each with four blocks of a story task and four blocks of a math task. The average length of the blocks was 30s, with the length of the math blocks matching the length of the story blocks. In the story blocks participants were presented with brief auditory adapted stories from Aesop’s fables followed by a two-alternative forced-choice question asking participants about the topic of the story. In the math blocks participants were presented with arithmetic operations followed by “equals” and then two choices. The operations are presented auditorily and the participants responded by pushing a button.

Relational Processing

The relational processing task (henceforth “relational”) was an adaptation of a task developed by Smith, Keramatian, & Christoff (2007) designed to localize activation in anterior prefrontal cortex. Participants were presented with two pairs of stimuli, one at

the top of the screen and one at the bottom, that may differ across two dimensions: shape or texture. They were asked to decide whether the top pair of objects differs in shape or texture. After they decided, they were asked whether the bottom pair of objects differs in the same dimension as the top pair. In the control matching condition, they were presented with two objects at the top of the screen and one at the bottom. In the middle of the screen they either saw the word “shape” or the word “texture”. They were asked to decide whether the bottom object matches either of the top ones in the dimension mentioned in the middle of the screen. For both conditions, subjects respond “yes” or “no” with button press. The task has two runs, with three relational, three control, and three fixation blocks. In the relational block there are four trials with the stimuli presented for 3500ms with a 500ms ITI, while in the control block there are five trials with the stimuli presented for 2800ms with an ITI of 400ms.

Emotion Processing

The emotion processing task (henceforth “emotion”) was adapted from the one developed by Hariri et al. (2006). Participants were presented with either three faces or three shapes on the screen, one at the top and two at the bottom and were asked to match the bottom face or shape to the ones in the top. The faces had either a fearful or an angry expression. The task had two runs, with three face and three shape blocks each and 8s of fixation at the end of each run. Each block was preceded by a 3000ms task cue (“shape” or “face”) and had six trials with the stimuli presented for 2000ms with a 1000ms ITI. Both the emotion and the ToM task require some degree of ToM. The ToM task asks participants to implement mental state attributions when watching the geometrical shapes interact, hence the ToM is intentional. On the other hand, the emotion task has a far

smaller degree of ToM as participants only implicitly attribute mental states to the faces they view (Kliemann & Adolphs, 2018; Van Overwalle & Vandekerckhove, 2013).

Image Preprocessing

The imaging data used in this dissertation were the “minimally preprocessed” included in the WU-Minn HCP Consortium S900 Release (WU - Minn Consortium Human Connectome Project, 2015). The dMRI data preprocessing included echo planar imaging (EPI) distortion, eddy-current-induced distortion, and subject motion correction, gradient nonlinearity correction, normalization of the b0 image intensity across runs, and registering the mean b0 volume to a native T1 volume. The tfMRI data had undergone spatial artifact/distortion correction, cross-modal registration, and spatial normalization to MNI space. Additionally, we further processed the dMRI data with FSL’s BEDPOSTX multi-shell, ball and zeppelins model (Hernández et al., 2013; Sotiropoulos et al., 2016) to model white matter fiber orientations and crossing fibers, and removed motion artifacts from the tfMRI data using ICA-AROMA (Griffanti et al., 2014; Pruim, Mennes, Buitelaar, & Beckmann, 2015; Pruim et al., 2015). All fMRI data were spatially smoothed at 4mm.

Regions of Interest Definition

We used two sets of ROIs for our analyses: one set in the cerebrum and one in the cerebellum. The cerebral brain areas from which ROIs were extracted included anterior temporal lobe (ATL), dorsomedial prefrontal cortex (DMPFC), precuneus (PreC), temporoparietal junction (TPJ), and ventromedial prefrontal cortex (VMPFC). Portions of the ATL are considered to be a repository for person-related semantic knowledge, social concepts, and social scripts (Olson et al., 2007; Ross & Olson, 2010; Wang et al., 2017).

The DMPFC is believed to be involved in reasoning about others' enduring traits (e.g. stable attitudes, preferences, and dispositions) (Schurz & Perner, 2015; Van Overwalle, 2009; Van Overwalle & Baetens, 2009; Van Overwalle & Vandekerckhove, 2013), while the VMPFC is known to represent emotional and motivational components of social reasoning, linking valence to particular persons, their actions, and their thoughts (Koster-Hale et al., 2017; Molenberghs et al., 2016). The PreC has been suggested to be linked with mental imagery related to perspective taking (e.g. online mental simulation of how a person thinks, acts or behaves in fictitious situations) (Cavanna & Trimble, 2006; Peer et al., 2015; Schiller et al., 2009; Schurz et al., 2014; Uddin et al., 2007) and the TPJ is thought to be involved in attributing other's transient mental states (e.g. instant goals, thoughts, and feelings) (Koster-Hale & Saxe, 2013; Van Overwalle, 2009). Although other brain areas are considered to support the mentalizing network (occipital gyrus, fusiform gyrus, amygdala, inferior frontal gyrus), we focused on brain areas involved in basic, core social processes. To ensure sensitivity within each individual we defined individual-specific ROIs using the social cognition task as a ToM ROI localizer. To precisely localize each ToM ROI, the social cognition task was processed on the "grayordinate-based" space (cortical surface vertices and subcortical voxels) using the MSM-All registration (Robinson et al., 2014). We used the Connectome Workbench software (Marcus et al., 2011) to manually extract the vertices (which were later transformed to MNI coordinates) of the peak activations of the bilateral ten predefined ROIs (as well as their magnitudes) from the contrast "ToM > random" (socially meaningful interaction of the shapes > random movement of the shapes) for each individual separately. These individual-specific cluster peak coordinates were used as

input (spheres, 6 mm radius) for subsequent seed-based brain connectivity analyses at the individual level (probabilistic tractography and PPI). It is important to note that, based on the meta-analysis by (Schurz et al., 2014), which showed that activation from social or intentional interactions > physical movements contrast spans broadly on the TPJ, the TPJ was defined as a broad brain area encompassing the inferior parietal lobule (IPL, i.e. perspective taking) and posterior superior temporal sulcus (pSTS, i.e. biological motion perception). In the event that the TPJ had multiple clusters (falling either into what is traditionally considered to be the TPJ, or IPL or pSTS), we selected the strongest cluster to avoid excessive inter-subject inconsistency.

For the ROIs in the cerebellum we used a different approach. Although several studies have attempted to functionally map the cerebellar cortex (Buckner et al., 2011; Diedrichsen & Zotow, 2015; Guell, Gabrieli, et al., 2018; Guell, Schmahmann, et al., 2018; King et al., 2019; Krienen & Buckner, 2009; Marek et al., 2018; Riedel et al., 2015), there isn't consensus when it comes to clear boundaries within the cerebellum that correspond to specific functions. Hence, it was impossible to employ the same approach as we did with the cerebral ROIs since there was no predefined cerebellar areas that are identified as playing specific roles in specific functions. Following the method used by Guell, Gabrieli, and Schmahmann (2018) we transformed individual level 2 cope files (results of within-subject fixed-effects grayordinate-based analyses which generate output files that index mean effects for an individual subject averaged across the two scan runs for a task) into Cohen's d group maps by first transforming the grayordinate .dscalar.nii files to NIFTI. We then used FSL commands `fsselectvols` to extract the contrast of interest "ToM > random" for each individual, and `fslmerge, fsmaths -Tmean, -Tstd, and -`

div to merge the individual contrast images, extract the mean, and the standard deviation, and divide the two, ultimately getting group Cohen's D maps for the contrasts "ToM > random" (ToM), "faces > shapes" (emotion), "story > math" (language), "2-back > 0-back" (working memory), "reward > punishment" (gambling), "relational > match" (relational processing), and "average" (motor) based on our 671 subjects. The HCP S900 Release provides level 3 group z-maps, but Cohen's D maps made it possible to observe the effect size of each task contrast rather than the significance of the BOLD signal change. A sample of 671 subjects ensures that a d value higher than 0.5 (J. Cohen, 1988) will be statistically significant even after correction for multiple comparisons ($d = z/\sqrt{n}$, $d > 0.5$ we have $z > 12.95$ for $n = 671$; analysis of 17,853 cerebellar voxels would require $p < 0.000028$ after Bonferroni correction, and $p < 0.000028$ is equivalent to $z > 4.026$). Accordingly, we used the Cohen's D maps and a threshold of 0.5 to extract clusters of activation for each task and local maxima within each cluster. After using a whole cerebellar mask to retain only the clusters and local maxima within the cerebellum, clusters smaller than 100 mm^3 were further removed in order to omit very small clusters that were considered to be non-informative and would make a comprehensive description of the results too extensive. The coordinates of the remainder local maxima from the "ToM > random" (ToM) contrast within the cerebellum were used to create group cerebellar ROIs (spheres, 6 mm radius). Eleven ROIs were created for the left cerebellar hemisphere and seven ROIs were created for the right.

Cluster Overlap and Euclidean distances

Given that the HCP dataset uses FNIRT registration to the MNI template, we calculated the percentage of overlap of each cerebellar cluster, in reference to the

cerebellar lobules, by using Diedrichsen's FNIRT MNI maximum probability map (Diedrichsen et al., 2009). It has been shown though that functional parcellation of the cerebellum does not match its anatomical parcellation into lobules (King et al., 2019). Because of this, we created an atlas of cerebellar lobes (anterior, posterior, flocculonodular, and vermis) by combining the lobules from Diedrichsen's FNIRT MNI maximum probability map (Diedrichsen et al., 2009) that belong in each lobe and used these maps for our analyses. We used FSL's atlasq tool to determine the percentage of overlap of each cerebellar cluster to the cerebellar lobes, hence determining the primary location of each cluster. The Sørensen–Dice coefficient, which is a statistic measuring the similarity of two samples (Dice, 1945; Sørensen, 1948), was then used to calculate the percentage of overlap between the functional clusters generated from all tasks and determine their similarity, and Euclidean distances were calculated to estimate the distances of local maxima within and between clusters. At the individual level, we thresholded Z-scored β -weights of each subject's activation map for each task to > 0 to retain only increased activation during the tasks and then ran Wilcoxon signed-rank tests between each task pair to examine whether there was a statistical difference between them.

Psychophysiological Interaction Analyses

Effective connectivity is a way to capture stimulus-driven patterns of directional influence among neural areas (Friston et al., 1997). Along with functional connectivity, they are the two ways to quantify functional integration (Friston, 1994). As functional connectivity only expresses statistical dependencies (i.e. non-directional correlations) among spatially segregated neuronal events (Stephan & Friston, 2010), we selected

effective connectivity which describes the directed causal influences of brain regions, simply the *effect* of one region on another (Zeidman et al., 2019). PPI analyses were used as a method of understanding effective connectivity by identifying brain regions whose activity depends on an interaction between psychological context (the task) and physiological state (the time course of brain activity) of the seed region (Gerchen, Bernal-Casas, & Kirsch, 2014; O'Reilly, Woolrich, Behrens, Smith, & Johansen-Berg, 2012; Smith, Gseir, Speer, & Delgado, 2016). To address Hypothesis 2, we built a generalized PPI model (McLaren et al., 2012) using a non-deconvolution method (Di & Biswal, 2017) for each cerebellar and cerebral ROI. Our model had five separate regressors: two psychological regressors of task events (mental interaction and random interaction), one physiological regressor of the time series of the seed ROIs and two corresponding interaction regressors (task events \times seed ROI's time series). To estimate the effective connectivity, we used the contrast between the interaction regressors (PPI mental > PPI random). *Z*-scored β -weights were extracted for each pair of cerebellar to cerebral ROIs, which resulted in an 11 x 5 matrix for the left cerebellar-right cerebral hemispheres and a 7 x 5 matrix for the right cerebellar-left cerebral hemispheres for each individual. We applied symmetrization to the matrices by averaging the *Z*-scored β -weights of each pair of cerebro-cerebellar and cerebello-cerebral ROIs (Tompson et al., 2020). At the group level of the effective connectivity, one-sample t-tests were performed across individuals at each pair of ROIs to detect any significant effective connectivity. What we expect to learn from this analysis is which cerebellar ToM regions present significant coupling with cerebral ToM regions due to mental state attribution (ToM task).

Diffusion Analyses

Probabilistic tractography analyses were performed using FSL's probtrackx2 (probabilistic tracking with crossing fibres) (Behrens et al., 2003, 2007) in each subject's native space and then the results were transformed to MNI standard space. An ROI-to-ROI approach was used with cerebral and cerebellar ROIs used as seeds and targets to reconstruct each subject's cerebello-cerebral white matter connections. Fiber tracking was initialized in both directions separately (from seed to target and vice versa) and 5,000 streamlines were drawn from each voxel in each ROI. To address Hypothesis 3, tractographies were performed to delineate the cerebello-thalamo-cortical (CTC) (Middleton & Strick, 1997; Palesi et al., 2017; Schmahmann & Pandya, 1997) and cortico-ponto-cerebellar (CPC) (Palesi et al., 2017; Ramnani, 2006) between left/right cerebral hemispheres and right/left cerebellar hemispheres. For the CTC tractographies, a binarized mask of the superior cerebellar peduncle in MNI space from the Johns Hopkins University ICBM-DTI-81 white-matter labels atlas (Hua et al., 2018; Mori, S., Wakana, S., Van Zijl, P. C., & Nagae-Poetscher, 2005; Wakana et al., 2007) was used as a waypoint, while the binarized contralateral cerebellar and cerebral hemispheres were set as exclusion masks (Example: CTC tractography between a left cerebellar ROI and a right cerebral ROI would entail a left superior cerebellar peduncle waypoint, a right cerebellar hemisphere exclusion mask, and a left cerebral hemisphere exclusion mask). For the CPC tractographies, a binarized mask of the middle cerebellar peduncle in MNI space from the Johns Hopkins University ICBM-DTI-81 white-matter labels atlas (Hua et al., 2018; Mori, S., Wakana, S., Van Zijl, P. C., & Nagae-Poetscher, 2005; Wakana et al., 2007) was used as a waypoint, and the contralateral cerebellar and cerebral hemispheres

were used as exclusion masks (Example: CPC tractography between a left cerebellar ROI and a right cerebral ROI would entail the middle cerebellar peduncle waypoint mask, a right cerebellar hemisphere exclusion mask, and a left cerebral hemisphere exclusion mask). The pons was not selected as an inclusion mask due to lack of a pons mask in standardized space through a standardized atlas. We also chose not to include the thalamus as a waypoint mask for the CTC pathway to keep the CTC and CPC tractography methods as similar as possible.

The number of streamlines for each path, produced by tractography, was obtained and used as a white matter integrity measurement.

Brain-behavior Association

Spearman correlations were used to examine brain-behavior association and address Hypothesis 4. The brain features used were streamline counts for all left cerebellar-right cerebral and right cerebellar-left cerebral ROI-ROI connections. For the behavior, we used two metrics from the HCP ToM task: task accuracy (Social_Task_TOM_Perc_TOM) and median reaction time (Social_Task_Median_RT_TOM).

CHAPTER 3

RESULTS

Testing Hypothesis 1: Functions of Distinct Cerebellar Regions

We first tested the hypothesis that regions of the cerebellum have domain specific functions. At the group level, we extracted clusters of activation related to different task domains (Figure 2) and local maxima (Figure 3) for each task.

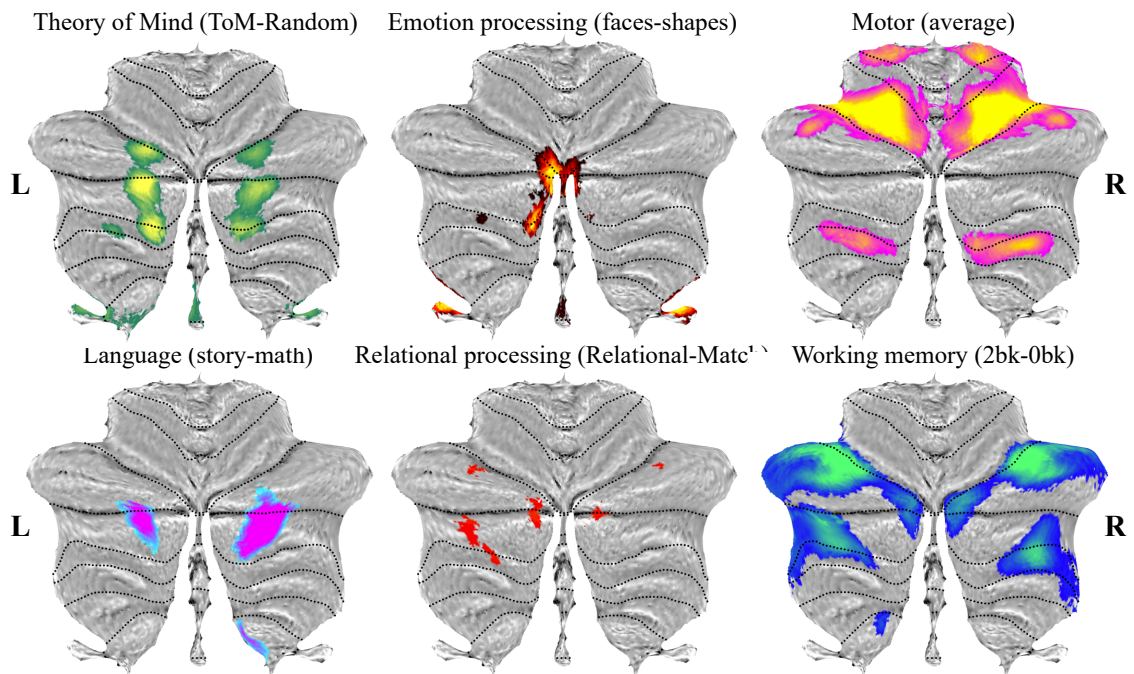


Figure 2. Group-level task clusters of activation. Clusters of activation at the group level for the six fMRI tasks: Theory of Mind, emotion processing, motor, language, relational processing, and working memory.

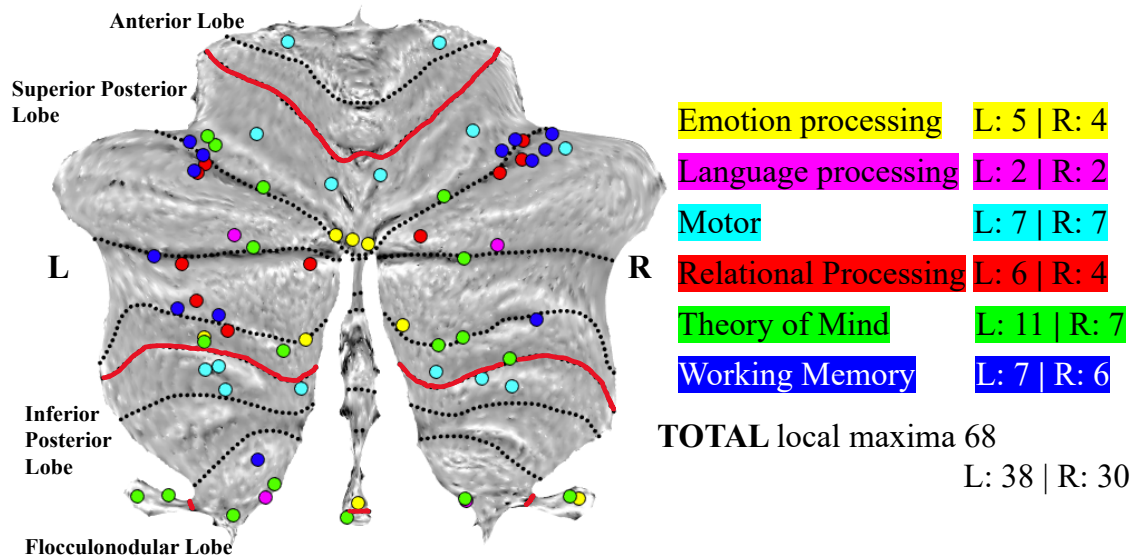


Figure 3. Local maxima for each functional task. Cerebellar flatmap with local maxima of each functional task. Each colored circle corresponds to a functional task. The total amount of local maxima among all tasks and the amount within each task is indicated next to the name of the tasks. Yellow=emotion processing; Pink=language processing; Turquoise=motor; Red=relational processing; Green=theory of mind; Blue=working memory; L=left; R=right.

The Sørensen–Dice coefficient was used to calculate the overlap between the functional clusters of all tasks. Euclidean distances were then calculated to estimate the distances of local maxima within and between clusters. Lastly, at the individual level, we performed Wilcoxon signed-rank tests for each task pair to examine whether there was a statistical difference between them. All task contrasts generated activation clusters at the Cohen’s $d > 0.5$ threshold, except for the gambling task which was, subsequently, excluded from all analyses. Percentage of overlap between functional clusters from the tasks and cerebellar lobes are presented in Table 1. Consistent with previous findings, the motor task was the only task that activated the anterior lobe (lobules I–VI), while emotion and ToM were the only tasks showing activation in the vermis (Albazron et al., 2019; Brady et al., 2019; Gao et al., 2018; Watson et al., 2019). Interestingly, ToM and emotion tasks also

activated the flocculonodular lobe (lobule X), an area of the cerebellum known to regulate saccadic eye movements and balance (B. Cohen & Highstein, 1972; Ito, 1982; Schniepp et al., 2017). A detailed description of the overlap of each cluster of activation and each lobule is presented in Table A1.

Table 1. Activation clusters and cerebellar lobe percent overlap. The amount of overlap between task activation clusters and cerebellar lobes expressed in percentage. The percentages in each row do not add up to 100% as part of the activations were categorized as “Unknown”. Percentages in bold are > 10%.

Task \ Cerebellar lobe	Anterior	Posterior	Flocculonodular	Vermis
Emotion	0.002	62.54	9.07	18.56
Language		92.83	0.01	0.38
Motor	17.04	71.35	0.004	1.96
Relational		95.98		0.13
ToM	0.0008	87.96	1.91	2.98
Working Memory	0.03	91.14	0.02	0.73

Percentage of overlap between activation clusters, calculated using the Sørensen–Dice coefficient, is presented in Table 2. The ToM and language clusters share almost half of their voxels (45.17%), the ToM and emotion clusters share 18.66% of their voxels, and ToM and working memory clusters share 11.76% of their voxels, while working memory shares voxels with the motor (20.99%) and relational processing (19.61%). The language and motor clusters were the only ones with zero overlap. The remainder of the clusters have <10% overlap. To further examine the relationship

Table 2. Percentage of overlap between activation clusters. Percentages in bold are >10%.

Task	Emotion	Language	Motor	Relational Processing	ToM	Working Memory
Emotion						
Language	0.09					
Motor	1.08	0				
Relational Processing	8.37	0.63	1.09			
ToM	18.66	45.17	5.50	2.89		
Working Memory	7.50	0.41	20.99	19.61	11.76	

between the task clusters of activation, we extracted the local maxima within each cluster and then calculated the mean Euclidean distance of the local maxima within each cluster and between clusters. More than 96% of Euclidean distances were >8.5mm (whole sample of Euclidean distances $M = 39.01$, $SD = 8.41$) which is 78 proximal Euclidean distances out of 2278. Out of those, 58 are Euclidean distances of local maxima between different clusters, bringing the percentage of local maxima that are proximal, yet belong to dissociable clusters, to 2.5%. These findings demonstrate that at the group level there isn't strong evidence to make a claim of generality vs specificity for cerebellar function, even though Euclidean distances results indicate that, despite shared activation, overlapping clusters have distinct local maxima.

At the individual level, we extracted average positive beta-weights for each subject and each task. Kolmogorov-Smirnov tests indicated that the task beta-weights did not follow a normal distribution (all p 's < .001; Table A2) hence we used Spearman's rho

to examine the strength and direction of association between each task, and the Wilcoxon signed-rank test to examine whether there was a statistical difference between each task pair. We found very weak positive correlations between emotion-language, emotion-relational, emotion-ToM, working memory-motor and working memory-language beta-weights, and a weak correlation between relational-working memory beta-weights (Table A3). Wilcoxon signed-rank tests showed that there was a statistically significant difference between beta-weights of all task pairs (Table A4) except for the relational-emotion pair. Together, the group-level and individual-level findings suggest that the cerebellum functions in a domain specific way with distinct cerebellar areas devoted to distinct cognitive functions.

Testing Hypothesis 2: Effective Connectivity between ToM Cerebellum and Cerebrum

Our second hypothesis was that functionally-defined ToM regions in the cerebellum would functionally interact with functionally-defined contralateral ToM regions in the cerebrum. Our goal was to map the ToM cerebellocerebral effective connectivity patterns. To achieve this, we created 6mm spherical ROIs based on each ToM local maximum (Figure 4) and individual-subject peak activation on the ToM task for ATL, DMPFC, PreC, TPJ, and VMPFC. We used PPI to examine the effective connectivity between the cerebellar and cerebral ToM areas. This resulted in 110 connections between the left cerebellum and right cerebrum (55 cerebellum-to-cerebrum e.g. L1 to R_ATL, L1 to R_DMPFC, 55 cerebrum-to-cerebellum e.g. R_ATL to L1, R_DMPFC to L1) and 70 connections between the right cerebellum and left cerebrum (35 CTC, 35 CPC). We extracted Z -scored β -weights for each pair of cerebellar to contralateral cerebral ROIs for each subject, averaged them, and at the group level we

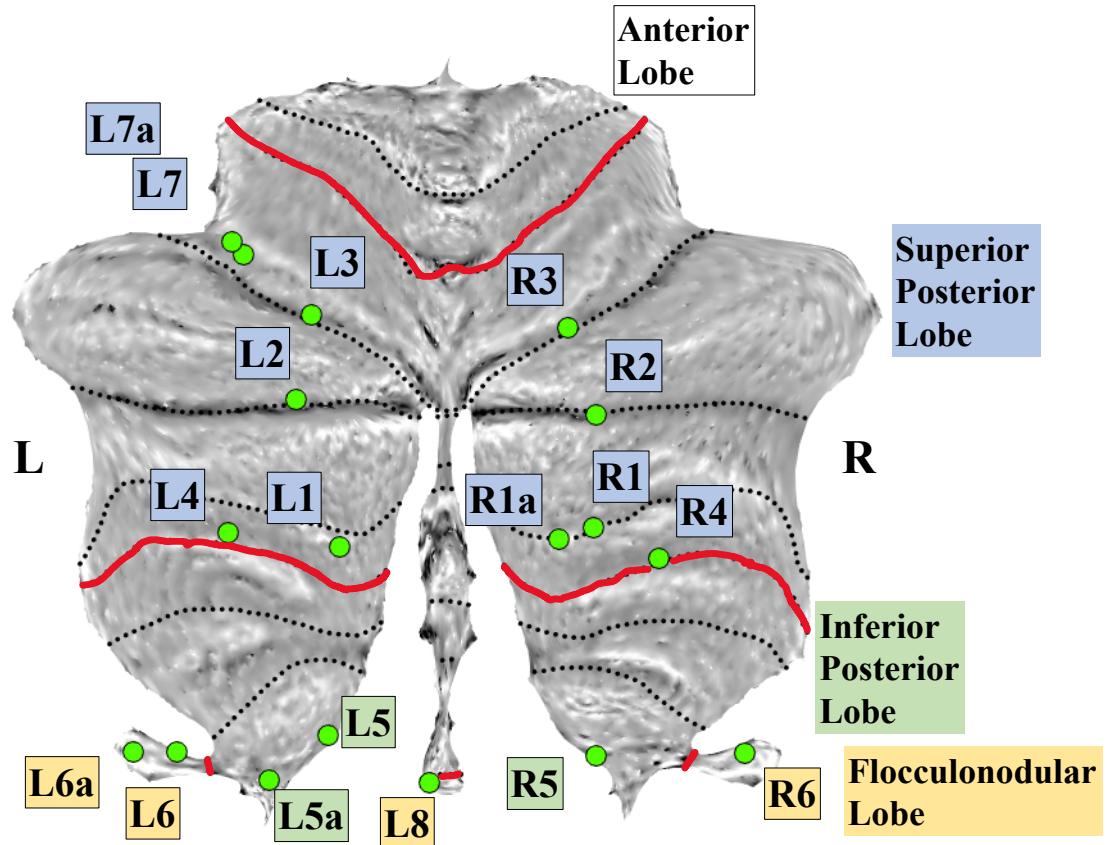


Figure 4. Data-driven cerebellar ToM local maxima. If a local maximum was found in both cerebellar hemispheres, it was named accordingly (e.g. L1 – R1). If two local maxima were found in close proximity, the extra local maximum was denoted by the letter “a”. L=left; R=right.

performed one-sample t-tests at each pair of ROIs to detect significant effectivity connectivity. Each local maximum was represented in both cerebellar hemispheres and named accordingly (e.g. L1 – R1) with the exception of left hemisphere local maxima L7, L7a, and L8. In some cases, two local maxima were found in close proximity. In these cases we gave the extra local maximum the same name as the one near it, adding “a”. This resulted in the pairs L5-L5a (Euclidean distance = 8.485), L6-L6a (Euclidean distance = 7.211), L7-L7a (Euclidean distance = 4.899), and R1-R1a (Euclidean distance = 6.325). We asked whether these cerebellar local maxima with close proximity to one

another had different effective connectivity to and from ToM ROIs in the cerebrum. The goal of this was to understand whether these ROIs have any functional distinction. To test this, we ran paired samples t-tests (Wilcoxon signed-rank tests for connections that did not follow a normal distribution) on individual beta-weights for all connections between proximal ROIs (e.g. paired t-test comparing L5-ATL to L5a-ATL). Effective connectivity results for all R1 – R1a pairs was not significant but we found significant results between some proximal left ROIs (see Tables A5 & A6). These findings suggest that there is significantly different effective connectivity between ToM cerebellar and cerebral ROIs despite close proximity of the cerebellar local maxima.

Overall, we found more connections (Figure 5) and stronger effective connectivity (Figure 6) between the left cerebellum and right cerebrum compared to the right cerebellum and the left cerebrum. Local maxima on each of the right cerebellar lobes were connected to all five ToM cerebral areas. On the left cerebellar hemisphere all local maxima ROIs were significantly connected to three or more contralateral cerebral ROIs, with the exception of L8 on the flocculonodular node which was only connected to the right ATL and DMPFC. The right DMPFC, ATL, and TPJ displayed significant connections with most left cerebellar ROIs (10 out of 11 left cerebellar ROIs for the DMPFC and 9 out of 11 for the ATL and TPJ; Figure 6a). The right cerebellar hemisphere displayed a different pattern of connectivity. With the exception of R1 and R1a, which combined were significantly connected to all left cerebral ROIs, all other right cerebellar ROIs were significantly connected to either one or two left cerebral ROIs. The left TPJ was the brain area with significant effective connectivity from all right cerebellar ROIs, except R_4. Combining the significant connections of all the left

cerebellar ROIs, we find that the left superior posterior, inferior posterior, and flocculonodular lobes each displays significant connectivity to all five right ToM brain areas. The right superior posterior cerebellar lobe is significantly connected to all five left cerebral brain areas if we combine the significant connectivity results of all its cerebellar ROIs (R1-R4), but the right inferior posterior lobe is only connected to the left ATL and TPJ and the right flocculonodular lobe is only connected to the left TPJ (Figure 6b).

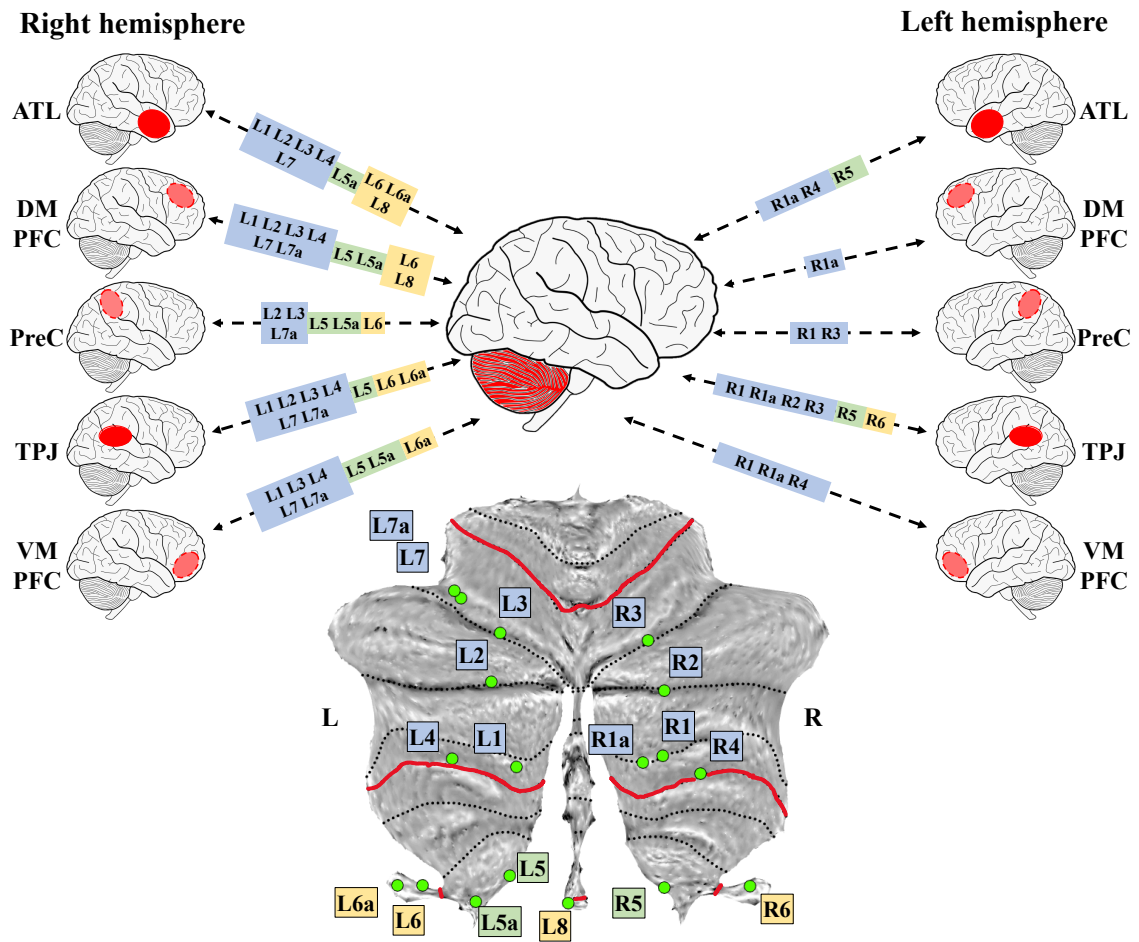


Figure 5. Effective connectivity between cerebellar and cerebral ToM ROIs. Blue = superior posterior lobe; Green = inferior posterior lobe; Yellow = flocculonodular lobe; ATL = anterior temporal lobe; DMPFC = dorsomedial prefrontal cortex; PreC = precuneus; TPJ = temporoparietal junction; VMPFC = ventromedial prefrontal cortex; L = left; R = right.

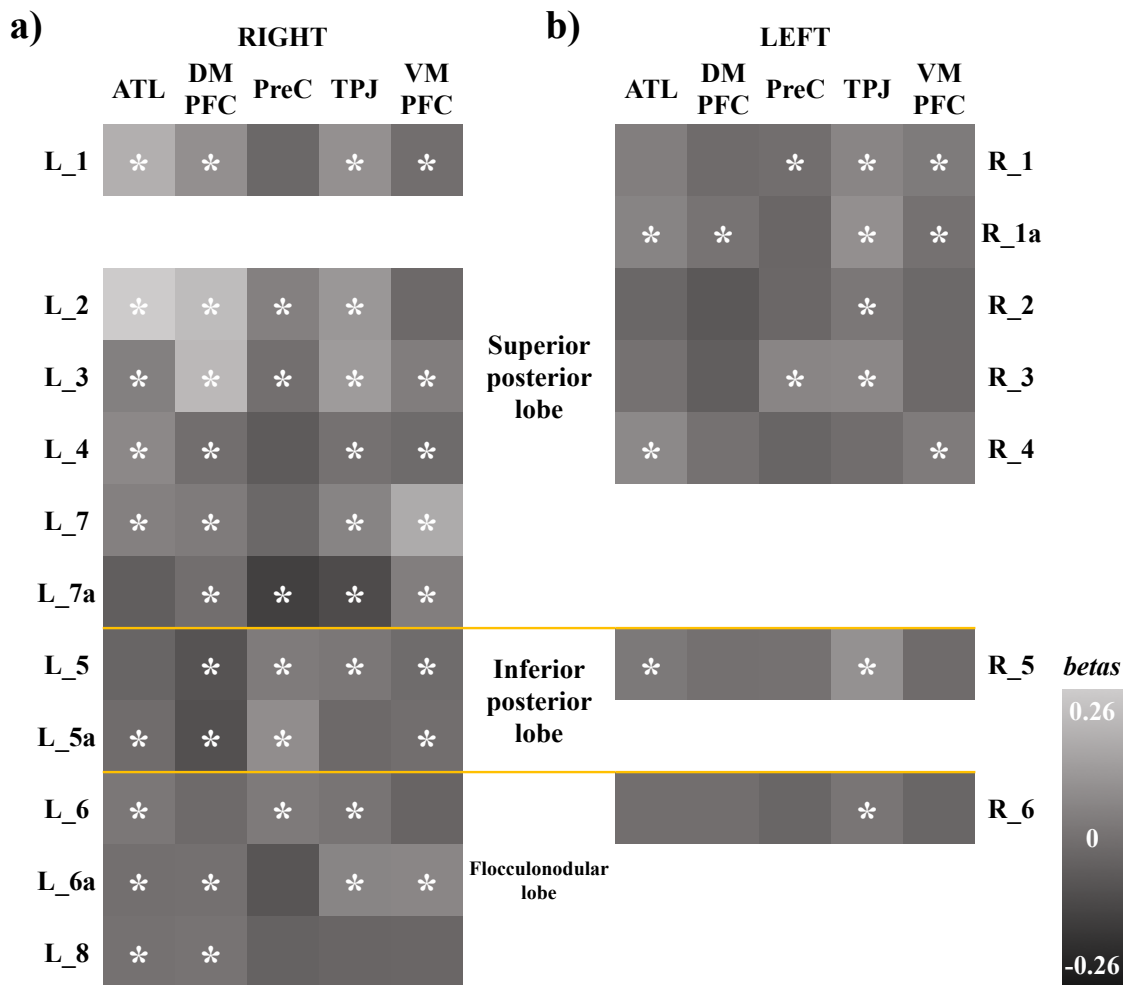


Figure 6. Effective connectivity significance between cerebellar and cerebral ToM ROIs. Stars indicate significant connections. ATL = anterior temporal lobe; DMPFC = dorsomedial prefrontal cortex; PreC = precuneus; TPJ = temporoparietal junction; VMPFC = ventromedial prefrontal cortex.

All the above results indicate that there is a clear functional connection between ToM cerebellar and cerebral areas and there seems to be a difference in the connectivity pattern between cerebellar hemispheres but also between cerebellar lobes with the left cerebellar lobes communicating with all right ToM cerebral areas and the right cerebellum displaying a more active posterior lobe. Notably, local maxima in both cerebellar hemispheres showed strongest connectivity to the TPJ, while the right DMPFC

was significantly connected to all left local maxima whereas the left DMPFC was weakly connected only to R1a local maximum.

Testing Hypothesis 3: Structural Connectivity between ToM Cerebellum and Cerebrum

Our third hypothesis was that the cerebellar ToM areas would be structurally connected to cerebral ToM areas. To test this, we ran probabilistic tractography to reconstruct the CTC and CPC white matter pathways. We used the same 6mm spherical ROIs from the PPI analysis as seeds and targets for the tractographies, the superior cerebellar peduncle as a waypoint for the CTC white matter pathway, and the middle cerebellar peduncle for the CPC white matter pathway. We then extracted streamline counts for each pathway.

The average streamline count spanned from 0.93 (L_ATL to R5; Table A7) to 211.01 (L8 to R_DMPFC; Table A8). Overall, the right and left CTC and CPC pathways showed similar connectivity patterns and average streamline counts (Figure 7).

We combined the individual average streamline counts to create average streamline counts for the superior posterior, inferior posterior, and flocculonodular lobes for the right and left CTC and CPC pathways (Table 3). Kolmogorov-Smirnov tests indicated that the white matter pathway streamline counts did not follow a normal distribution (all p 's < .001; Table A9) hence we used Spearman's rho to examine the strength and direction of association between left and right CTCs and CPCs, and the Wilcoxon signed-rank test to examine whether there was a statistical difference between them. For both the CTC and CPC pathways we found that the right superior posterior

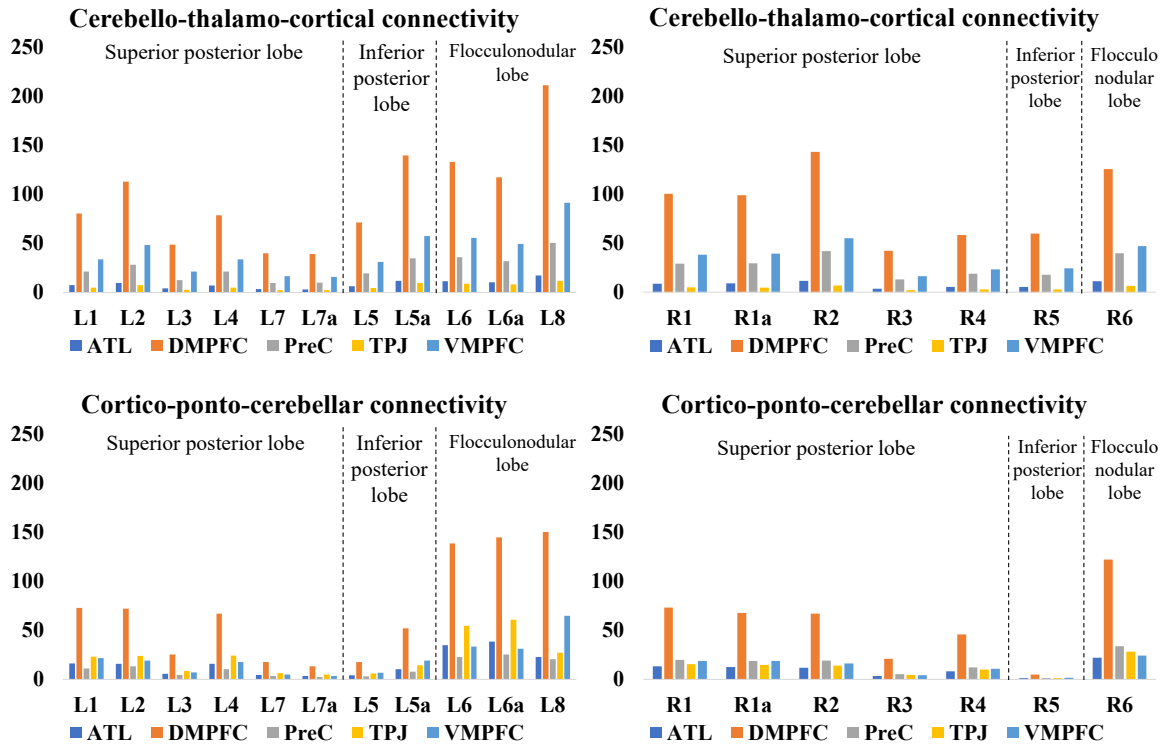


Figure 7. Mean streamline counts for each cerebello-thalamo-cortical and cortico-ponto-cerebellar white matter tract. Average ToM CTC and CPC streamline counts per local maximum. ATL = anterior temporal lobe; DMPFC = dorsomedial prefrontal cortex; PreC = precuneus; TPJ = temporoparietal junction; VMPFC = ventromedial prefrontal cortex

streamline count is correlated to the left superior posterior, inferior, and flocculonodular lobes but it shows greater correlation to the left superior posterior lobe. The same applies for the inferior posterior and flocculonodular lobe streamline counts for both the right and left cerebellar hemisphere (Tables A10 & A11). Wilcoxon signed-rank tests showed that there was a statistically significant difference in streamline counts between each lobe pair (e.g. left superior posterior – right superior posterior) for CTC and CPC tracks, with the majority of subjects having greater CTC streamline counts in the right superior posterior lobe rather than the left but smaller streamline counts in the right inferior and flocculonodular lobes compared to the respective left. The exact same pattern

Table 3. Mean cerebello-thalamo-cortical (CTC) and cortico-ponto-cerebellar (CPC) streamline counts. Average ToM CTC and CPC streamline counts per cerebellar hemisphere and lobe. The average streamline counts of whole ToM CTC and CPC pathways are in bold.

	Streamline count			Streamline count	
	Mean	SD		Mean	SD
Left CTC	35.52	(23.07)	Right CTC	32.76	(22.77)
Left superior posterior lobe	24.27	(18.79)	Right superior posterior lobe	32.26	(24.54)
Left inferior posterior lobe	38.42	(30.75)	Right inferior posterior lobe	22.04	(23.65)
Left flocculonodular lobe	56.10	(34.66)	Right flocculonodular lobe	45.99	(32.48)
Left CPC	28.04	(20.64)	Right CPC	21.74	(17.01)
Left superior posterior lobe	17.82	(13.45)	Right superior posterior lobe	20.89	(16.80)
Left inferior posterior lobe	13.96	(12.94)	Right inferior posterior lobe	1.86	(2.71)
Left flocculonodular lobe	57.84	(44.96)	Right flocculonodular lobe	45.87	(48.06)

The exact same pattern was observed in the CPC tracks as well (Table A12). We also found that the overall left CTC streamline count was significantly larger compared to the right CTC streamline count and the same was true for the CPCs (Table A12).

Additionally, we found that CTC streamline counts (from the left and right cerebellar hemispheres) were significantly larger compared to the ipsilateral CPC streamline counts

(Table A12). CTC pathways from both the left and right cerebellar hemisphere and towards all five contralateral ToM cerebral ROIs displayed the exact same streamline count pattern (DMPFC>VMPFC>PreC>ATL>TPJ). The CPC pathways did not display an equally homogenous pattern. In the CPC pathways projecting to the left cerebellar hemisphere, the TPJ was the brain area with the second largest streamline count towards all cerebellar ROIs, except for L8. Also, in the CPC pathways projecting to the right cerebellar hemisphere, the VMPFC displayed disproportionately smaller streamline counts towards all right cerebellar ROIs compared both to the CTC patterns and the left CPC pattern (Figure 7; Tables A7 & A8). Overall, the DMPFC was the cerebral area with the greatest streamline count among both the CTC and CPC pathways.

The above results point to a structural connection between the ToM cerebellar and cerebral areas. The feedforward (CTC) and feedback (CPC) pathway streamlines counts between the right and left cerebellar lobes differ significantly with the right superior posterior lobe having a greater streamline count than the left, but the left having significantly greater streamline counts in the inferior and flocculonodular lobes. The DMPFC appeared to be the ToM brain area with the largest streamline count from and to it.

Testing Hypothesis 4: Brain-behavior Association

We used Spearman's rho to examine the strength and direction of association between each white matter connectivity metric and behavior measurements. Our analysis showed that the participants demonstrated ceiling effects for both ToM measurements (task accuracy: skewness = -2.16, task speed: skewness = 1.03). We found some

significant correlations between the behavioral ToM indices and CTC and CPC white matter connectivity, but none survived multiple comparison corrections using FDR.

CHAPTER 4

DISCUSSION

The cerebellum is an underappreciated brain structure for which little is still known. For decades it was considered to contribute solely to motor functions, hence the vast majority of cerebellar research is related to movement. Evidence regarding the cerebellum's potential role on other functions, such as cognition and emotion, started slowly emerging in the past two decades, and only in the past few years researchers have started taking a more active interest in examining these contributions in depth. In this study we ventured to explore the cerebellum's role in ToM, the ability to attribute mental states to others and interpret their intentions, perspectives, and beliefs. We used a large-scale dataset and mapped out the cerebellum's functional and structural profiles in relation to ToM.

First, we investigated whether the cerebellum is functionally specific. At the group level, we found small overlap between the clusters of activation of the six tasks (emotion processing, language, motor, relational processing, ToM, working memory). ToM had a sizeable overlap with the emotion and language. The ToM-emotion overlap occurred in the vermis and bilateral flocculonodular lobes (Figure 2) and was anticipated. The vermis and flocculonodular lobes have been considered the limbic system of the cerebellum (Schmahmann, 1994), involved in affective behavior through their structural connections to the amygdala, hippocampus, septum (Heath & Harper, 1974; Snider et al., 1976) and hypothalamus (Hu et al., 2008). Vermal stimulation in mice, cats, and primates leads to fire pattern modulation in these structures (Babb, Mitchell, & Crandall, 1974; Berman, 1997; Bobée, Mariette, Tremblay-Leveau, & Caston, 2000; Zanchetti &

Zoccolini, 1954) and aggression amelioration in human patients (Heath et al., 1979). Damage to the vermis has been shown to lead to atypical social and emotional behaviors (Levisohn et al., 2000; Manto & Mariën, 2015; Pollack, 1997; Schmahmann, 1991; Schmahmann & Sherman, 1998; Tavano et al., 2007) and neuroimaging studies have confirmed that the vermis and flocculonodular lobes are active during emotion learning or change of affect tasks (Beauregard et al., 1998; Gündel et al., 2003; Lane et al., 1997) and social processing (Guell, Gabrieli, et al., 2018; Van Overwalle et al., 2014). This overlap also makes sense due to the emotion task itself which has a degree of ToM, albeit implicit, by attributing emotion to the faces viewed. Emotion attribution from faces is considered key to social cognition (Hoche et al., 2016) but this task has been shown to require less ToM compared to the ToM task (Wang et al., 2020). The ToM-language overlap, on the other hand, was expected mainly due to the nature of the language task used. The adapted stories from Aesop's fables that the participants heard during scanning involved animals or humans interacting in easily understandable social situations (Binder et al., 2011). Hence, we believe it is the social aspect of the stories that may have activated ToM areas as well, leading to the overlap.

It is important to note that the clusters, and subsequently their overlap, are heavily dependent on thresholding decisions. Guell et al. (2018) also used the HCP S900 dataset to examine the task representations on the cerebellum but they analyzed the 2mm smoothed fMRI data. Subsequently, their task clustering results are similar to ours, but the cluster overlaps are smaller. Specifically, they reported only an overlap between the ToM and language tasks. Complimented by the resting-state functional connectivity analysis they performed, they conclude that the cerebellum has domain-specific

representations of different kinds of cognition and emotion. We believe this is a reasonable conclusion, but we wanted to provide additional evidence which would strengthen the claim to a domain-specific cerebellar role.

The task cluster overlaps led us to explore in more depth the relationship between the activation clusters. We extracted local maxima within each task and calculated Euclidean distances among local maxima within clusters of a task and between clusters of different tasks. We found that in spite of the overlap, each cluster had distinct local maxima, not proximal to the ones in the overlapping clusters. These results add to the notion that the cerebellum operates in a functionally specific way. Lastly, we analyzed the beta-weights for each task at the individual level and found that all pairs, except for relational processing and emotion, have a significantly different pattern of activation. Overall, our results provide support to our hypothesis that the cerebellum functions in a domain-specific manner.

Second, we mapped the ToM cerebellocerebral effective connectivity patterns by running PPI analyses between the cerebellar and cerebral (ATL, DMPFC, PreC, TPJ, VMPFC) ToM areas. We found important cerebellar hemispherical differences in effective connectivity. The left cerebellar hemisphere displayed more and stronger effective connections to the contralateral cerebral ToM areas compared to the right cerebellar hemisphere. These results fit well with our current knowledge of the mentalizing network's organization in the brain. The mentalizing network is a right brain hemisphere dominated network (Wang et al., 2020) with multiple studies showing right ATL (Acres et al., 2009; Gainotti, 2007; Olson et al., 2007, 2013; Rice et al., 2015) and right TPJ (Karolis et al., 2019; Santiesteban et al., 2015; Saxe, 2010; Saxe & Wexler,

2005; Van Overwalle & Baetens, 2009) lateralization for tasks involving social stimuli, though there are mixed findings for the latter. In our study, the ATL displayed this lateralization with the right ATL being significantly connected to all but two left ToM cerebellar ROIs. Interestingly, the TPJ did not display lateralizing effects since the TPJs bilaterally displayed significant connectivity to the respective, contralateral cerebellar ToM ROIs. The role of the TPJs in ToM is debated with several studies showing unilateral right TPJ activation in ToM (see above), but others showing bilateral involvement (Bzdok et al., 2012; Gallagher et al., 2000; Jenkins & Mitchell, 2010; Molenberghs et al., 2016; Schurz et al., 2014; Van Overwalle, 2009). Despite this debate, we attribute the bilateral TPJ activation to the fact that the ToM task involved videos of socially meaningful motions. In their study on the underlying neural responses of anthropomorphism in autism spectrum disorder and typically developing individuals, Ammons et al. (2018) found bilateral TPJ activation during observation of social movement regardless of the type of agent (human figure or geometrical shape) in both autistic and typically developing individuals. Furthermore, in our study the used a broader definition of the TPJ which could include parts of the IPL, known to be involved in perspective taking and pSTS, suggests involvement in biological motion perception. We believe that the nature of the stimuli used to activate the ToM areas (shapes interacting in a socially meaningful way vs neutrally), combined with our selection method of the TPJ ROI, could explain the significant bilateral cerebellar connectivity to almost all local maxima to the contralateral TPJs. To sum up, our results show a laterality effect of ToM cerebellar connections which match the laterality effects observed in functional activation of the cerebral areas involved in ToM processing.

Third, we examined the structural connectivity profile between cerebellar and cerebral ToM areas. We recreated the CTC and CPC pathways using probabilistic tractography. We found that the bilateral CTC pathways had greater streamline counts compared to the CPC pathways. Furthermore, the CTC and CPC pathways from and to the left cerebellum had greater streamline counts compared to the right CTC and CPC pathways. This result matches nicely with our effective connectivity results and with the known literature of the mentalizing network being a right brain hemisphere dominated network. The ToM streamline count pattern, with the DMPFC and VMPFC leading in average streamline counts, is partially concurrent to the effective connectivity findings. It is the TPJ that is effectively connected to more cerebellar ToM ROIs, followed by the DMPFC, the ATL, and then the VMPFC, but the well-known quantitative mismatch between structural and functional connectivity (Huang & Ding, 2016) could explain why even though the DMPFC and VMPFC lead in average streamline counts they aren't also the top ones with effective connectivity to most ToM cerebellar ROIs.

Lastly, we examined whether the streamline count of the CTC and CPC pathways correlated with the behavior indices of ToM. We used speed and accuracy of the ToM task the participants completed during their MRI scan. We found no correlation after FDR correction for multiple comparisons. We believe this is attributed to ceiling effects for the two behavioral ToM indices due to the fact that this task was originally designed for autistic children (Castelli et al., 2002), making it potentially easy for neurotypical adults.

Limitations and Future Directions

This study has a few limitations. First, connectivity analyses are inherently vulnerable to conceptual and methodological issues (Buckner et al., 2013) and their results depend on various factors (e.g. ROI selection methods, stimuli features, thresholding choices). Accordingly, our findings should be interpreted with caution (Turchi et al., 2018; Uddin et al., 2008). Furthermore, diffusion MRI tractography has received criticism for being a method with high rates of false positives (Maier-Hein et al., 2017; Reveley et al., 2015; Thomas et al., 2014). Regardless, functional and diffusion MRI have provided valuable insight into the anatomical and functional organization of the ToM network, and as both techniques improve, we hope other researchers replicate and extend our cerebellar findings.

Secondly, our study could incorporate the ipsilateral ToM cerebello-cerebral effective and structural connections to include a more complete image of the ToM cerebello-cerebral connectome. Additionally, further analyses could be included between the ToM cerebellar areas and a set of non-ToM cerebral areas (e.g. motor) to serve as control analyses.

Lastly, as with other large-scale publicly available datasets, the HCP does not include the optimal stimuli for activation of the ToM cerebellar and cerebral areas. The social animation task was originally designed to assess ToM in children with autism spectrum disorder (Castelli et al., 2002). Hence, the task may have been easy for neurotypical adults, leading to ceiling effects making it impossible to capture individual differences between the cerebrocerebellar white matter microstructure and behavior. Future studies could develop more ecologically valid social tasks (Redcay & Schilbach,

2019; Schilbach et al., 2013) to be able to capture the variation in ToM cerebellocerebral connectivity and behavior.

Conclusions

This multimodal neuroimaging study investigated the structural and functional connectivity between ToM cerebellar and cerebral areas. We found that the cerebellum functions in a domain specific way with distinct cerebellar areas devoted to distinct cognitive functions, among which is ToM. Furthermore, we mapped out the effective connectivity between the ToM cerebellum and cerebrum and found cerebellar hemispherical differences in cerebello-cerebral effective connectivity. The left cerebellar hemisphere displayed more and stronger effective connections to the contralateral cerebral ToM areas. Additionally, we recreated the CTC and CPC pathways using probabilistic tractography and found that the CTC and CPC pathways from and to the left cerebellum had greater streamline counts compared to the right CTC and CPC pathways. We also found that the bilateral CTC pathways had greater streamline counts compared to the CPC pathways. Lastly, we examined the relationship between CTC and CPC white matter and speed and accuracy on the ToM task but found no correlation, possibly due to ceiling effects while performing the ToM.

REFERENCES CITED

- Ackermann, H., Wildgruber, D., Daum, I., & Grodd, W. (1998). *Does the cerebellum contribute to cognitive aspects of speech production? A functional magnetic resonance imaging (fMRI) study in humans.*
- Acres, K., Taylor, K. I., Moss, H. E., Stamatakis, E. A., & Tyler, L. K. (2009). Complementary hemispheric asymmetries in object naming and recognition: A voxel-based correlational study. *Neuropsychologia*, *47*(8–9), 1836–1843.
<https://doi.org/10.1016/j.neuropsychologia.2009.02.024>
- Albazron, F. M., Bruss, J., Jones, R. M., Yock, T. I., Pulsifer, M. B., Cohen, A. L., Nopoulos, P. C., Abrams, A. N., Sato, M., & Boes, A. D. (2019). Pediatric postoperative cerebellar cognitive affective syndrome follows outflow pathway lesions. *Neurology*, *93*(16), E1561–E1571.
<https://doi.org/10.1212/WNL.00000000000008326>
- Ammons, C. J., Doss, C. F., Bala, D., & Kana, R. K. (2018). Brain Responses Underlying Anthropomorphism, Agency, and Social Attribution in Autism Spectrum Disorder. *The Open Neuroimaging Journal*, *12*(1), 16–29.
<https://doi.org/10.2174/1874440001812010016>
- Amodio, D. M., & Frith, C. D. (2006). Meeting of minds: The medial frontal cortex and social cognition. *Nature Reviews Neuroscience*, *7*(4), 268–277.
<https://doi.org/10.1038/nrn1884>
- Babb, T. L., Mitchell, A. G., & Crandall, P. H. (1974). Fastigiobulbar and dentatohalamic influences on hippocampal cobalt epilepsy in the cat. *Electroencephalography and Clinical Neurophysiology*, *36*(C), 141–154.

[https://doi.org/10.1016/0013-4694\(74\)90151-5](https://doi.org/10.1016/0013-4694(74)90151-5)

Bailey, A., Luthert, P., Dean, A., Harding, B., Janota, I., Montgomery, M., Rutter, M., & Lantos, P. (1998). A clinicopathological study of autism. *Brain*, *121*(5), 889–905.

<https://doi.org/10.1093/brain/121.5.889>

Barch, D. M., Burgess, G. C., Harms, M. P., Petersen, S. E., Schlaggar, B. L., Corbetta, M., Glasser, M. F., Curtiss, S., Dixit, S., Feldt, C., Nolan, D., Bryant, E., Hartley, T., Footer, O., Bjork, J. M., Poldrack, R., Smith, S., Johansen-Berg, H., Snyder, A. Z., & Van Essen, D. C. (2013). Function in the human connectome: Task-fMRI and individual differences in behavior. *NeuroImage*, *80*, 169–189.

<https://doi.org/10.1016/j.neuroimage.2013.05.033>

Beauregard, M., Leroux, J. M., Bergman, S., Arzoumanian, Y., Beaudoin, G., Bourgouin, P., & Stip, E. (1998). The functional neuroanatomy of major depression: An fMRI study using an emotional activation paradigm. *NeuroReport*, *9*(14), 3253–3258.

<https://doi.org/10.1097/00001756-199810050-00022>

Beer, J. S., & Ochsner, K. N. (2006). Social cognition: A multi level analysis. *Brain Research*, *1079*(1), 98–105. <https://doi.org/10.1016/J.BRAINRES.2006.01.002>

Behrens, T. E. J., Berg, H. J., Jbabdi, S., Rushworth, M. F. S., & Woolrich, M. W. (2007). Probabilistic diffusion tractography with multiple fibre orientations: What can we gain? *NeuroImage*, *34*(1), 144–155.

<https://doi.org/10.1016/j.neuroimage.2006.09.018>

Behrens, T. E. J., Woolrich, M. W., Jenkinson, M., Johansen-Berg, H., Nunes, R. G., Clare, S., Matthews, P. M., Brady, J. M., & Smith, S. M. (2003). Characterization and Propagation of Uncertainty in Diffusion-Weighted MR Imaging. *Magnetic*

- Resonance in Medicine*, 50(5), 1077–1088. <https://doi.org/10.1002/mrm.10609>
- Benjamini, Y., & Hochberg, Y. (1995). Controlling the False Discovery Rate : A Practical and Powerful Approach to Multiple Testing. *Journal of the Royal Statistical Society*, 57(1), 289–300.
- Binder, J. R., Gross, W. L., Allendorfer, J. B., Bonilha, L., Chapin, J., Edwards, J. C., Grabowski, T. J., Langfitt, J. T., Loring, D. W., Lowe, M. J., Koenig, K., Morgan, P. S., Ojemann, J. G., Rorden, C., Szaflarski, J. P., Tivarus, M. E., & Weaver, K. E. (2011). Mapping anterior temporal lobe language areas with fMRI: A multicenter normative study. *NeuroImage*, 54(2), 1465–1475. <https://doi.org/10.1016/j.neuroimage.2010.09.048>
- Blakemore, S. J. (2008). The social brain in adolescence. In *Nature Reviews Neuroscience* (Vol. 9, Issue 4, pp. 267–277). Nature Publishing Group. <https://doi.org/10.1038/nrn2353>
- Bobée, S., Mariette, E., Tremblay-Leveau, H., & Caston, J. (2000). Effects of early midline cerebellar lesion on cognitive and emotional functions in the rat. *Behavioural Brain Research*, 112, 107–117.
- Brady, R. O., Gonsalvez, I., Lee, I., Öngür, D., Seidman, L. J., Schmahmann, J. D., Eack, S. M., Keshavan, M. S., Pascual-Leone, A., & Halko, M. A. (2019). Cerebellar-prefrontal network connectivity and negative symptoms in schizophrenia. *American Journal of Psychiatry*, 176(7), 512–520. <https://doi.org/10.1176/appi.ajp.2018.18040429>
- Brodal, P., & Bjaalie, J. G. (1997). Salient anatomic features of the cortico-ponto-cerebellar pathway. *Progress in Brain Research*, 114, 227–250.

[https://doi.org/10.1016/s0079-6123\(08\)63367-1](https://doi.org/10.1016/s0079-6123(08)63367-1)

Buckner, R. L., Krienen, F. M., Castellanos, A., Diaz, J. C., & Yeo, B. T. T. (2011). The organization of the human cerebellum estimated by intrinsic functional connectivity. *Journal of Neurophysiology*, *106*(5), 2322–2345.

<https://doi.org/10.1152/jn.00339.2011>

Buckner, R. L., Krienen, F. M., & Yeo, B. T. T. (2013). Opportunities and limitations of intrinsic functional connectivity MRI. In *Nature Neuroscience* (Vol. 16, Issue 7, pp. 832–837). Nature Publishing Group. <https://doi.org/10.1038/nn.3423>

Bzdok, D., Heeger, A., Langner, R., Laird, A. R., Fox, P. T., Palomero-Gallagher, N., Vogt, B. A., Zilles, K., & Eickhoff, S. B. (2015). Subspecialization in the human posterior medial cortex. *NeuroImage*, *106*, 55–71.

<https://doi.org/10.1016/j.neuroimage.2014.11.009>

Bzdok, D., Langner, R., Schilbach, L., Jakobs, O., Roski, C., Caspers, S., Laird, A. R., Fox, P. T., Zilles, K., & Eickhoff, S. B. (2013). Characterization of the temporo-parietal junction by combining data-driven parcellation, complementary connectivity analyses, and functional decoding. *NeuroImage*, *81*, 381–392.

<https://doi.org/10.1016/j.neuroimage.2013.05.046>

Bzdok, D., Schilbach, L., Vogeley, K., Schneider, K., Laird, A. R., Langner, R., & Eickhoff, S. B. (2012). Parsing the neural correlates of moral cognition: ALE meta-analysis on morality, theory of mind, and empathy. *Brain Structure and Function*, *217*(4), 783–796. <https://doi.org/10.1007/s00429-012-0380-y>

Castelli, F., Frith, C., Happe, F., & Frith, U. (2002). Autism, Asperger syndrome and brain mechanisms for the attribution of mental states to animated shapes. *Brain*, *125*,

1839–1849.

Castelli, F., Happé, F., Frith, U., & Frith, C. (2000). Movement and mind: A functional imaging study of perception and interpretation of complex intentional movement patterns. *NeuroImage*, *12*(3), 314–325. <https://doi.org/10.1006/nimg.2000.0612>

Catani, M., Jones, D. K., Daly, E., Embiricos, N., Deeley, Q., Pugliese, L., Curran, S., Robertson, D., & Murphy, D. G. M. (2008). Altered cerebellar feedback projections in Asperger syndrome. *NeuroImage*, *41*(4), 1184–1191. <https://doi.org/10.1016/J.NEUROIMAGE.2008.03.041>

Cavanna, A. E., & Trimble, M. R. (2006). The precuneus: A review of its functional anatomy and behavioural correlates. In *Brain* (Vol. 129, Issue 3, pp. 564–583). Oxford University Press. <https://doi.org/10.1093/brain/awl004>

Clower, D. M., Dum, R. P., & Strick, P. L. (2005). Basal ganglia and cerebellar inputs to “AIP.” *Cerebral Cortex*, *15*(7), 913–920. <https://doi.org/10.1093/cercor/bhh190>

Cohen, B., & Highstein, S. M. (1972). Cerebellar Control of the Vestibular Pathways to Oculomotor Neurons. *Progress in Brain Research*, *37*(C), 411–425. [https://doi.org/10.1016/S0079-6123\(08\)63916-3](https://doi.org/10.1016/S0079-6123(08)63916-3)

Cohen, J. (1988). Statistical Power Analysis for the Behavioural Science (2nd Edition). In *Statistical Power Analysis for the Behavioral Sciences* (Vol. 3, Issue 2). <http://repositorio.unan.edu.ni/2986/1/5624.pdf>

Courchesne, E., Townsend, J., Akshoomoff, N. A., Saitoh, O., Yeung-Courchesne, R., Lincoln, A. J., James, H. E., Haas, R. H., Schreibman, L., & Lau, L. (1994). Impairment in shifting attention in autistic and cerebellar patients. *Behavioral Neuroscience*, *108*(5), 848–865. <https://doi.org/10.1037/0735-7044.108.5.848>

- Delbello, M. P., Strakowski, S. M., Zimmerman, M. E., Hawkins, J. M., & Sax, K. W. (1999). MRI analysis of the cerebellum in bipolar disorder: A pilot study. *Neuropsychopharmacology*, *21*(1), 63–68. [https://doi.org/10.1016/S0893-133X\(99\)00026-3](https://doi.org/10.1016/S0893-133X(99)00026-3)
- Delgado, M. R., Nystrom, L. E., Fissell, C., Noll, D. C., & Fiez, J. A. (2000). Tracking the hemodynamic responses to reward and punishment in the striatum. *Journal of Neurophysiology*, *84*(6), 3072–3077. <https://doi.org/10.1152/jn.2000.84.6.3072>
- Desmond, J. E., Gabrieli, J. D. E., Wagner, A. D., Ginier, B. L., & Glover, G. H. (1997). Lobular patterns of cerebellar activation in verbal working-memory and finger-tapping tasks as revealed by functional MRI. *Journal of Neuroscience*, *17*(24), 9675–9685. <https://doi.org/10.1523/jneurosci.17-24-09675.1997>
- Di, X., & Biswal, B. B. (2017). Psychophysiological interactions in a visual checkerboard task: Reproducibility, reliability, and the effects of deconvolution. *Frontiers in Neuroscience*, *11*(OCT), 573. <https://doi.org/10.3389/fnins.2017.00573>
- Dice, L. R. (1945). Measures of the Amount of Ecologic Association Between Species. *Ecology*, *26*(3), 297–302. <https://doi.org/10.2307/1932409>
- Diedrichsen, J., & Zotow, E. (2015). Surface-Based Display of Volume-Averaged Cerebellar Imaging Data. *PLOS ONE*, *10*(7), e0133402. <https://doi.org/10.1371/journal.pone.0133402>
- Dum, R. P., & Strick, P. L. (2003). An Unfolded Map of the Cerebellar Dentate Nucleus and its Projections to the Cerebral Cortex. *Journal of Neurophysiology*, *89*(1), 634–639. <https://doi.org/10.1152/jn.00626.2002>
- Fiez, J. A., Petersen, S. E., Cheney, M. K., & Raichle, M. E. (1992). Impaired non-motor

- learning and error detection associated with cerebellar damage: A single case study. *Brain*, 115(1), 155–178. <https://doi.org/10.1093/brain/115.1.155>
- Fiez, J. A., & Raichle, M. E. (1997). Linguistic processing. *International Review of Neurobiology*, 41, 233–254. [https://doi.org/10.1016/s0074-7742\(08\)60354-2](https://doi.org/10.1016/s0074-7742(08)60354-2)
- Fine, E. J., Ionita, C. C., & Lohr, L. (2002). The history of the development of the cerebellar examination. *Seminars in Neurology*, 22(4), 375–384. <https://doi.org/10.1055/s-2002-36759>
- Friston, K J, Buechel, C., Fink, G. R., Morris, J., Rolls, E., & Dolan, R. J. (1997). Psychophysiological and modulatory interactions in neuroimaging. *NeuroImage*, 6(3), 218–229. <https://doi.org/10.1006/nimg.1997.0291>
- Friston, Karl J. (1994). Functional and effective connectivity in neuroimaging: A synthesis. *Human Brain Mapping*, 2(1–2), 56–78. <https://doi.org/10.1002/hbm.460020107>
- Frith, C. D., & Frith, U. (2006). The Neural Basis of Mentalizing. In *Neuron* (Vol. 50, Issue 4, pp. 531–534). Cell Press. <https://doi.org/10.1016/j.neuron.2006.05.001>
- Frith, C. D., & Frith, U. (2007). Social Cognition in Humans. In *Current Biology* (Vol. 17, Issue 16, pp. R724–R732). Cell Press. <https://doi.org/10.1016/j.cub.2007.05.068>
- Frith, C. D., & Frith, U. (2012). Mechanisms of social cognition. *Annual Review of Psychology*, 63, 287–313. <https://doi.org/10.1146/annurev-psych-120710-100449>
- Gainotti, G. (2007). Different patterns of famous people recognition disorders in patients with right and left anterior temporal lesions: A systematic review. In *Neuropsychologia* (Vol. 45, Issue 8, pp. 1591–1607). Pergamon. <https://doi.org/10.1016/j.neuropsychologia.2006.12.013>

- Gallagher, H. L., Happé, F., Brunswick, N., Fletcher, P. C., Frith, U., & Frith, C. D. (2000). Reading the mind in cartoons and stories: An fMRI study of “theory of mind” in verbal and nonverbal tasks. *Neuropsychologia*, *38*(1), 11–21. [https://doi.org/10.1016/S0028-3932\(99\)00053-6](https://doi.org/10.1016/S0028-3932(99)00053-6)
- Gao, Z., Davis, C., Thomas, A. M., Economo, M. N., Abrego, A. M., Svoboda, K., De Zeeuw, C. I., & Li, N. (2018). A cortico-cerebellar loop for motor planning. *Nature*, *563*(7729), 113–116. <https://doi.org/10.1038/s41586-018-0633-x>
- Gerchen, M. F., Bernal-Casas, D., & Kirsch, P. (2014). Analyzing task-dependent brain network changes by whole-brain psychophysiological interactions: A comparison to conventional analysis. *Human Brain Mapping*, *35*(10), 5071–5082. <https://doi.org/10.1002/hbm.22532>
- Glasser, M. F., Sotiropoulos, S. N., Wilson, J. A., Coalson, T. S., Fischl, B., Andersson, J. L., Xu, J., Jbabdi, S., Webster, M., Polimeni, J. R., Van Essen, D. C., & Jenkinson, M. (2013). The minimal preprocessing pipelines for the Human Connectome Project. *NeuroImage*, *80*, 105–124. <https://doi.org/10.1016/j.neuroimage.2013.04.127>
- Glickstein, M. (1992). The cerebellum and motor learning. *Journal of Cognitive Neuroscience*, *2*(6), 802–806. <https://doi.org/10.1162/jocn.1990.2.2.69>
- Glickstein, M. (1993). Motor skills but not cognitive tasks. *Trends in Neurosciences*, *16*(11), 450–451. [https://doi.org/10.1016/0166-2236\(93\)90074-V](https://doi.org/10.1016/0166-2236(93)90074-V)
- Gottwald, B., Wilde, B., Mihajlovic, Z., & Mehdorn, H. M. (2004). Evidence for distinct cognitive deficits after focal cerebellar lesions. *Journal of Neurology, Neurosurgery and Psychiatry*, *75*(11), 1524–1531. <https://doi.org/10.1136/jnnp.2003.018093>

- Granziera, C., Schmahmann, J. D., Hadjikhani, N., Meyer, H., Meuli, R., Wedeen, V., & Krueger, G. (2009). Diffusion Spectrum Imaging Shows the Structural Basis of Functional Cerebellar Circuits in the Human Cerebellum In Vivo. *PLoS ONE*, *4*(4), e5101. <https://doi.org/10.1371/journal.pone.0005101>
- Griffanti, L., Salimi-Khorshidi, G., Beckmann, C. F., Auerbach, E. J., Douaud, G., Sexton, C. E., Zsoldos, E., Ebmeier, K. P., Filippini, N., Mackay, C. E., Moeller, S., Xu, J., Yacoub, E., Baselli, G., Ugurbil, K., Miller, K. L., & Smith, S. M. (2014). ICA-based artefact removal and accelerated fMRI acquisition for improved resting state network imaging. *NeuroImage*, *95*, 232–247. <https://doi.org/10.1016/j.neuroimage.2014.03.034>
- Gross-Tsur, V., Ben-Bashat, D., Shalev, R. S., Levav, M., & Sira, L. Ben. (2006). Evidence of a developmental cerebello-cerebral disorder. *Neuropsychologia*, *44*(12), 2569–2572. <https://doi.org/10.1016/j.neuropsychologia.2006.04.028>
- Guell, X., Gabrieli, J. D. E., & Schmahmann, J. D. (2018). Triple representation of language, working memory, social and emotion processing in the cerebellum: convergent evidence from task and seed-based resting-state fMRI analyses in a single large cohort. *NeuroImage*, *172*(August 2017), 437–449. <https://doi.org/10.1016/j.neuroimage.2018.01.082>
- Guell, X., Schmahmann, J. D., Gabrieli, J. D. E., & Ghosh, S. S. (2018). Functional gradients of the cerebellum. *ELife*, *7*, 1–22. <https://doi.org/10.7554/eLife.36652>
- Gündel, H., O'Connor, M.-F., Littrell, L., Fort, C., & Lane, R. D. (2003). Functional Neuroanatomy of Grief: An fMRI Study. *American Journal of Psychiatry*, *160*(11), 1946–1953. <https://doi.org/10.1176/appi.ajp.160.11.1946>

- Hariri, A. R., Brown, S. M., Williamson, D. E., Flory, J. D., De Wit, H., & Manuck, S. B. (2006). Preference for immediate over delayed rewards is associated with magnitude of ventral striatal activity. *Journal of Neuroscience*, *26*(51), 13213–13217. <https://doi.org/10.1523/JNEUROSCI.3446-06.2006>
- Hartwright, C. E., Hansen, P. C., & Apperly, I. A. (2016). Current knowledge on the role of the Inferior Frontal Gyrus in Theory of Mind – A commentary on Schurz and Tholen (2016). *Cortex*, *85*, 133–136. <https://doi.org/10.1016/j.cortex.2016.10.005>
- Heath, R. G., Franklin, D. E., Walker, C. F., & Keating, J. W. (1982). Cerebellar vermal atrophy in psychiatric patients. *Biological Psychiatry*, *17*(5), 569–583.
- Heath, R. G., Franklin, D., & Shraberg, D. (1979). Gross pathology of the cerebellum in patients diagnosed and treated as functional psychiatric disorders. *The Journal of Nervous and Mental Disease*, *167*(10), 585–592.
- Heath, R. G., & Harper, J. W. (1974). Ascending projections of the cerebellar fastigial nucleus to the hippocampus, amygdala, and other temporal lobe sites. *Experimental Neurology*, *45*(2), 268–287. [https://pdf.sciencedirectassets.com/272536/1-s2.0-S0014488600X01355/1-s2.0-0014488674901186/main.pdf?x-amz-security-token=AgoJb3JpZ2luX2VjEMr%2F%2F%2F%2F%2F%2F%2F%2F%2F%2FwEaCXVzLWVhc3QtMSJHMEUCIEtI3s3TV77Tuiebb0yQd62ELbuHpMWe69ch5AhF5wtC4AiEAxFFTRZzz2E5VP](https://pdf.sciencedirectassets.com/272536/1-s2.0-S0014488600X01355/1-s2.0-0014488674901186/main.pdf?x-amz-security-token=AgoJb3JpZ2luX2VjEMr%2F%2F%2F%2F%2F%2F%2F%2F%2F%2F%2FwEaCXVzLWVhc3QtMSJHMEUCIEtI3s3TV77Tuiebb0yQd62ELbuHpMWe69ch5AhF5wtC4AiEAxFFTRZzz2E5VP)
- Hernández, M., Guerrero, G. D., Cecilia, J. M., García, J. M., Inuggi, A., Jbabdi, S., Behrens, T. E. J., & Sotiropoulos, S. N. (2013). Accelerating Fibre Orientation Estimation from Diffusion Weighted Magnetic Resonance Imaging Using GPUs. *PLoS ONE*, *8*(4). <https://doi.org/10.1371/journal.pone.0061892>

- Hoche, F., Guell, X., Sherman, J. C., Vangel, M. G., & Schmammann, J. D. (2016). Cerebellar Contribution to Social Cognition. *Cerebellum*, *15*(6), 732–743. <https://doi.org/10.1007/s12311-015-0746-9>
- Hokkanen, L. S. K., Kauranen, V., Roine, R. O., Salonen, O., & Kotila, M. (2006). Subtle cognitive deficits after cerebellar infarcts. *European Journal of Neurology*, *13*(2), 161–170. <https://doi.org/10.1111/j.1468-1331.2006.01157.x>
- Hu, D., Shen, H., & Zhou, Z. (2008). Functional asymmetry in the cerebellum: A brief review. In *Cerebellum* (Vol. 7, Issue 3, pp. 304–313). Springer. <https://doi.org/10.1007/s12311-008-0031-2>
- Hua, K., Zhang, J., Wakana, S., Jiang, H., Li, X., Reich, D. S., Calabresi, P. A., Pekar, J. J., van Zijl, P. C. M., & Mori, S. (2018). Tract Probability Maps in Stereotaxic Spaces: Analyses of White Matter Anatomy and Tract-Specific Quantification. *Neuroimage*, *39*(1), 336–347. <https://doi.org/10.1016/j.neuroimage.2007.07.053>
- Huang, H., & Ding, M. (2016). Linking Functional Connectivity and Structural Connectivity Quantitatively: A Comparison of Methods. *Brain Connectivity*, *6*(2), 99–108. <https://doi.org/10.1089/brain.2015.0382>
- Ito, M. (1982). Cerebellar control of the vestibulo-ocular reflex--around the flocculus hypothesis. *Annual Review of Neuroscience*, *5*(1), 275–296. <https://doi.org/10.1146/annurev.ne.05.030182.001423>
- Ito, M. (1984). *The Cerebellum and Neural Control*. Raven.
- Ito, M. (2002). Historical review of the significance of the cerebellum and the role of purkinje cells in motor learning. *Annals of the New York Academy of Sciences*, *978*(1), 273–288. <https://doi.org/10.1111/j.1749-6632.2002.tb07574.x>

- Ito, M. (2008). Control of mental activities by internal models in the cerebellum. *Nature Reviews Neuroscience*, 9(Box 1), 304–313. <https://doi.org/10.1038/nrn2332>
- Jacobsen, L. K., Giedd, J. N., Berquin, P. C., Krain, A. L., Hamburger, S. D., Kumra, S., & Rapoport, J. L. (1997). Quantitative morphology of the cerebellum and fourth ventricle in childhood-onset schizophrenia. *American Journal of Psychiatry*, 154(12), 1663–1669. <https://doi.org/10.1176/ajp.154.12.1663>
- Jenkins, A. C., & Mitchell, J. P. (2010). Mentalizing under uncertainty: Dissociated neural responses to ambiguous and unambiguous mental state inferences. *Cerebral Cortex*, 20(2), 404–410. <https://doi.org/10.1093/cercor/bhp109>
- Jissendi, P., Baudry, S., & Balériaux, D. (2008). Diffusion tensor imaging (DTI) and tractography of the cerebellar projections to prefrontal and posterior parietal cortices: A study at 3T. *Journal of Neuroradiology*, 35(1), 42–50. <https://doi.org/10.1016/J.NEURAD.2007.11.001>
- Karavasilis, E., Christidi, F., Velonakis, G., Giavri, Z., Kelekis, N. L., Efstathopoulos, E. P., Evdokimidis, I., & Dellatolas, G. (2019). Ipsilateral and contralateral cerebro-cerebellar white matter connections: A diffusion tensor imaging study in healthy adults. *Journal of Neuroradiology*, 46(1), 52–60. <https://doi.org/10.1016/j.neurad.2018.07.004>
- Karolis, V. R., Corbetta, M., & Thiebaut de Schotten, M. (2019). The architecture of functional lateralisation and its relationship to callosal connectivity in the human brain. *Nature Communications*, 10(1), 1–9. <https://doi.org/10.1038/s41467-019-09344-1>
- Kelly, R. M., & Strick, P. L. (2003). Cerebellar loops with motor cortex and prefrontal

- cortex of a nonhuman primate. *The Journal of Neuroscience*, 23(23), 8432–8444.
<https://doi.org/23/23/8432> [pii]
- Keser, Z., Hasan, K. M., Mwangi, B. I., Kamali, A., Ucisik-Keser, F. E., Riascos, R. F., Yozbatiran, N., Francisco, G. E., & Narayana, P. A. (2015). Diffusion tensor imaging of the human cerebellar pathways and their interplay with cerebral macrostructure. *Frontiers in Neuroanatomy*, 9(April), 1–13.
<https://doi.org/10.3389/fnana.2015.00041>
- King, M., Hernandez-Castillo, C. R., Poldrack, R. A., Ivry, R. B., & Diedrichsen, J. (2019). Functional boundaries in the human cerebellum revealed by a multi-domain task battery. *Nature Neuroscience*, 22(8), 1371–1378.
<https://doi.org/10.1038/s41593-019-0436-x>
- Kliemann, D., & Adolphs, R. (2018). The social neuroscience of mentalizing: challenges and recommendations. *Current Opinion in Psychology*, 24, 1–6.
<https://doi.org/10.1016/j.copsyc.2018.02.015>
- Koster-Hale, J., Richardson, H., Velez, N., Asaba, M., Young, L., & Saxe, R. (2017). Mentalizing regions represent distributed, continuous, and abstract dimensions of others' beliefs. *NeuroImage*, 161, 9–18.
<https://doi.org/10.1016/j.neuroimage.2017.08.026>
- Koster-Hale, J., & Saxe, R. (2013). Theory of Mind: A Neural Prediction Problem. *Neuron*, 79(5), 836–848. <https://doi.org/10.1016/j.neuron.2013.08.020>
- Krienen, F. M., & Buckner, R. L. (2009). Segregated fronto-cerebellar circuits revealed by intrinsic functional connectivity. *Cerebral Cortex*, 19(10), 2485–2497.
<https://doi.org/10.1093/cercor/bhp135>

- Lahnakoski, J. M., Glerean, E., Salmi, J., Jääskeläinen, I. P., Sams, M., Hari, R., & Nummenmaa, L. (2012). Naturalistic fMRI Mapping Reveals Superior Temporal Sulcus as the Hub for the Distributed Brain Network for Social Perception. *Frontiers in Human Neuroscience*, 6(August), 1–14.
<https://doi.org/10.3389/fnhum.2012.00233>
- Lane, R. D., Reiman, E. M., Bradley, M. M., Lang, P. J., Ahern, G. L., Davidson, R. J., & Schwartz, G. E. (1997). Neuroanatomical correlates of pleasant and unpleasant emotion. *Neuropsychologia*, 35(11), 1437–1444. [https://doi.org/10.1016/S0028-3932\(97\)00070-5](https://doi.org/10.1016/S0028-3932(97)00070-5)
- Leiner, H. C., Leiner, A. L., & Dow, R. S. (1986). Does the Cerebellum Contribute to Mental Skills? *Behavioral Neuroscience*, 100(4), 443–454.
<https://doi.org/10.1037/0735-7044.100.4.443>
- Leiner, H. C., Leiner, A. L., & Dow, R. S. (1993). Cognitive and language functions of the human cerebellum. *Trends in Neurosciences*, 16(11), 444–447.
[https://doi.org/10.1016/0166-2236\(93\)90072-T](https://doi.org/10.1016/0166-2236(93)90072-T)
- Levisohn, L., Cronin-Golomb, A., & Schmahmann, J. D. (2000). Neuropsychological consequences of cerebellar tumour resection in children. Cerebellar cognitive affective syndrome in a paediatric population. *Brain*, 123(5), 1041–1050.
<https://doi.org/10.1093/brain/123.5.1041>
- Lippmann, S., Manshadi, M., Baldwin, H., Drasin, G., Rice, J., & Alrajeh, S. (1982). Cerebellar vermis dimensions on computerized tomographic scans of schizophrenic and bipolar patients. *American Journal of Psychiatry*, 139(5), 667–668.
<https://doi.org/10.1176/ajp.139.5.667>

- Mackie, S., Shaw, P., Lenroot, R., Pierson, R., Greenstein, D. K., Nugent, T. F., Sharp, W. S., Giedd, J. N., & Rapoport, J. L. (2007). Cerebellar development and clinical outcome in attention deficit hyperactivity disorder. *American Journal of Psychiatry*, *164*(4), 647–655. <https://doi.org/10.1176/ajp.2007.164.4.647>
- Maier-Hein, K. H., Neher, P. F., Houde, J.-C., Côté, M.-A., Garyfallidis, E., Zhong, J., Chamberland, M., Yeh, F.-C., Lin, Y.-C., Ji, Q., Reddick, W. E., Glass, J. O., Chen, D. Q., Feng, Y., Gao, C., Wu, Y., Ma, J., Renjie, H., Li, Q., ... Descoteaux, M. (2017). The challenge of mapping the human connectome based on diffusion tractography. *Nature Communications*, *8*(1), 1349. <https://doi.org/10.1038/s41467-017-01285-x>
- Manto, M., Bower, J. M., Conforto, A. B., Delgado-García, J. M., Da Guarda, S. N. F., Gerwig, M., Habas, C., Hagura, N., Ivry, R. B., Marien, P., Molinari, M., Naito, E., Nowak, D. A., Ben Taib, N. O., Pelisson, D., Tesche, C. D., Tilikete, C., & Timmann, D. (2012). Consensus paper: Roles of the cerebellum in motor control-the diversity of ideas on cerebellar involvement in movement. *Cerebellum*, *11*(2), 457–487. <https://doi.org/10.1007/s12311-011-0331-9>
- Manto, M., & Mariën, P. (2015). Schmahmann's syndrome - identification of the third cornerstone of clinical ataxiology. In *Cerebellum and Ataxias* (Vol. 2, Issue 1, pp. 1–5). BioMed Central Ltd. <https://doi.org/10.1186/s40673-015-0023-1>
- Mar, R. A. (2011). The neural bases of social cognition and story comprehension. *Annual Review of Psychology*, *62*, 103–134. <https://doi.org/10.1146/annurev-psych-120709-145406>
- Marcus, D. S., Harwell, J., Olsen, T., Hodge, M., Glasser, M. F., Prior, F., Jenkinson, M.,

- Laumann, T., Curtiss, S. W., & Van Essen, D. C. (2011). Informatics and data mining tools and strategies for the human connectome project. *Frontiers in Neuroinformatics*, 5(June), 1–12. <https://doi.org/10.3389/fninf.2011.00004>
- Marek, S., Siegel, J. S., Gordon, E. M., Raut, R. V., Gratton, C., Newbold, D. J., Ortega, M., Laumann, T. O., Adeyemo, B., Miller, D. B., Zheng, A., Lopez, K. C., Berg, J. J., Coalson, R. S., Nguyen, A. L., Dierker, D., Van, A. N., Hoyt, C. R., McDermott, K. B., ... Dosenbach, N. U. F. (2018). Spatial and Temporal Organization of the Individual Human Cerebellum. *Neuron*, 100(4), 977-993.e7. <https://doi.org/10.1016/j.neuron.2018.10.010>
- Martin, A., Haxby, J. V., Lalonde, F. M., Wiggs, C. L., & Ungerleider, L. G. (1995). Discrete cortical regions associated with knowledge of color and knowledge of action. *Science*, 270(5233), 102–105. <https://doi.org/10.1126/science.270.5233.102>
- McKay, N. S., Iwabuchi, S. J., Häberling, I. S., Corballis, M. C., & Kirk, I. J. (2017). Atypical white matter microstructure in left-handed individuals. *Laterality*, 22(3), 257–267. <https://doi.org/10.1080/1357650X.2016.1175469>
- McLaren, D. G., Ries, M. L., Xu, G., & Johnson, S. C. (2012). A generalized form of context-dependent psychophysiological interactions (gPPI): A comparison to standard approaches. *NeuroImage*, 61(4), 1277–1286. <https://doi.org/10.1016/j.neuroimage.2012.03.068>
- Middleton, F. A., & Strick, P. L. (1994). Anatomical Evidence for Cerebellar and Basal Ganglia Involvement in Higher Cognitive Function. In *New Series* (Vol. 266, Issue 5184).
- Middleton, F. A., & Strick, P. L. (1997). Cerebellar Output Channels. *International*

- Review of Neurobiology*, 41, 61–82. [https://doi.org/10.1016/S0074-7742\(08\)60347-5](https://doi.org/10.1016/S0074-7742(08)60347-5)
- Middleton, F. A., & Strick, P. L. (2001). Cerebellar projections to the prefrontal cortex of the primate. *The Journal of Neuroscience : The Official Journal of the Society for Neuroscience*, 21(2), 700–712. <https://doi.org/10.1523/JNEUROSCI.21-02-00700.2001>
- Mittleman, G., Goldowitz, D., Heck, D. H., & Blaha, C. D. (2008). Cerebellar modulation of frontal cortex dopamine efflux in mice: Relevance to autism and schizophrenia. *Synapse*, 62(7), 544–550. <https://doi.org/10.1002/syn.20525>
- Molenberghs, P., Johnson, H., Henry, J. D., & Mattingley, J. B. (2016). Understanding the minds of others: A neuroimaging meta-analysis. *Neuroscience and Biobehavioral Reviews*, 65(April), 276–291. <https://doi.org/10.1016/j.neubiorev.2016.03.020>
- Mori, S., Wakana, S., Van Zijl, P. C., & Nague-Poetscher, L. M. (2005). *MRI atlas of human white matter*. Elsevier. <https://doi.org/10.1002/cmr.a.20051>
- O'Reilly, J. X., Woolrich, M. W., Behrens, T. E. J., Smith, S. M., & Johansen-Berg, H. (2012). Tools of the trade: Psychophysiological interactions and functional connectivity. *Social Cognitive and Affective Neuroscience*, 7(5), 604–609. <https://doi.org/10.1093/scan/nss055>
- Oldfield, R. C. (1971). The assessment and analysis of handedness: The Edinburgh inventory. *Neuropsychologia*, 9(1), 97–113. [https://doi.org/10.1016/0028-3932\(71\)90067-4](https://doi.org/10.1016/0028-3932(71)90067-4)
- Olson, I. R., McCoy, D., Klobusicky, E., & Ross, L. A. (2013). Social cognition and the anterior temporal lobes: A review and theoretical framework. *Social Cognitive and*

- Affective Neuroscience*, 8(2), 123–133. <https://doi.org/10.1093/scan/nss119>
- Olson, I. R., Plotzker, A., & Ezzyat, Y. (2007). The Enigmatic temporal pole: A review of findings on social and emotional processing. *Brain*, 130(7), 1718–1731. <https://doi.org/10.1093/brain/awm052>
- Palesi, F., De Rinaldis, A., Castellazzi, G., Calamante, F., Muhlert, N., Chard, D., Tournier, J. D., Magenes, G., D'Angelo, E., & Wheeler-Kingshott, C. A. M. G. (2017). Contralateral cortico-ponto-cerebellar pathways reconstruction in humans in vivo: Implications for reciprocal cerebro-cerebellar structural connectivity in motor and non-motor areas. *Scientific Reports*, 7(1), 1–13. <https://doi.org/10.1038/s41598-017-13079-8>
- Palmen, S. J. M. C., Van Engeland, H., Hof, P. R., & Schmitz, C. (2004). Neuropathological findings in autism. In *Brain* (Vol. 127, Issue 12, pp. 2572–2583). Oxford Academic. <https://doi.org/10.1093/brain/awh287>
- Peer, M., Salomon, R., Goldberg, I., Blanke, O., & Arzy, S. (2015). Brain system for mental orientation in space, time, and person. *Proceedings of the National Academy of Sciences*, 112(35), 11072–11077. <https://doi.org/10.1073/pnas.1504242112>
- Petersen, S. E., Fox, P. T., Posner, M. I., Mintun, M., & Raichle, M. E. (1988). Positron emission tomographic studies of the cortical anatomy of single-word processing. *Nature*, 331(6157), 585–589. <https://doi.org/10.1038/331585a0>
- Petersen, S. E., Fox, P. T., Posner, M. I., Mintun, M., & Raichle, M. E. (1989). Positron emission tomographic studies of the processing of single words. *Journal of Cognitive Neuroscience*, 1(2), 153–170. <https://doi.org/10.1162/jocn.1989.1.2.153>
- Pollack, I. F. (1997). Posterior fossa syndrome. *International Review of Neurobiology*,

41, 411–732. [https://doi.org/10.1016/s0074-7742\(08\)60362-1](https://doi.org/10.1016/s0074-7742(08)60362-1)

Pruim, R. H. R., Mennes, M., Buitelaar, J. K., & Beckmann, C. F. (2015). Evaluation of ICA-AROMA and alternative strategies for motion artifact removal in resting state fMRI. *NeuroImage*, *112*, 278–287.

<https://doi.org/10.1016/j.neuroimage.2015.02.063>

Pruim, R. H. R., Mennes, M., van Rooij, D., Llera, A., Buitelaar, J. K., & Beckmann, C. F. (2015). ICA-AROMA: A robust ICA-based strategy for removing motion artifacts from fMRI data. *NeuroImage*, *112*, 267–277.

<https://doi.org/10.1016/j.neuroimage.2015.02.064>

Raichle, M. E., Fiez, J. A., Videen, T. O., Macleod, A. mary K., Pardo, J. V., Fox, P. T., & Petersen, S. E. (1994). Practice-related changes in human brain functional anatomy during nonmotor learning. *Cerebral Cortex*, *4*(1), 8–26.

<https://doi.org/10.1093/cercor/4.1.8>

Ramnani, N. (2006). The primate cortico-cerebellar system: Anatomy and function.

Nature Reviews Neuroscience, *7*(7), 511–522. <https://doi.org/10.1038/nrn1953>

Ravizza, S. M., McCormick, C. A., Schlerf, J. E., Justus, T., Ivry, R. B., & Fiez, J. A. (2006). Cerebellar damage produces selective deficits in verbal working memory.

Brain, *129*(2), 306–320. <https://doi.org/10.1093/brain/awh685>

Redcay, E., & Schilbach, L. (2019). Using second-person neuroscience to elucidate the mechanisms of social interaction. *Nature Reviews Neuroscience*, *20*(8), 495–505.

<https://doi.org/10.1038/s41583-019-0179-4>

Reiman, E. M., Lane, R. D., Ahern, G. L., Schwartz, G. E., Davidson, R. J., Friston, K. J., Yun, L. S., & Chen, K. (1997). Neuroanatomical correlates of externally and

- internally generated human emotion. *American Journal of Psychiatry*, *154*(7), 918–925. <https://doi.org/10.1176/ajp.154.7.918>
- Reiman, E. M., Raichle, M. E., Robins, E., Mintun, M. A., Fusselman, M. J., Fox, P. T., Price, J. L., & Hackman, K. A. (1989). Neuroanatomical Correlates of a Lactate-Induced Anxiety Attack. *Archives of General Psychiatry*, *46*(6), 493–500. <https://doi.org/10.1001/archpsyc.1989.01810060013003>
- Reveley, C., Seth, A. K., Pierpaoli, C., Silva, A. C., Yu, D., Saunders, R. C., Leopold, D. A., & Ye, F. Q. (2015). Superficial white matter fiber systems impede detection of long-range cortical connections in diffusion MR tractography. *Proceedings of the National Academy of Sciences of the United States of America*, *112*(21), E2820–E2828. <https://doi.org/10.1073/pnas.1418198112>
- Rice, G. E., Ralph, M. A. L., & Hoffman, P. (2015). The roles of left versus right anterior temporal lobes in conceptual knowledge: An ALE meta-analysis of 97 functional neuroimaging studies. *Cerebral Cortex*, *25*(11), 4374–4391. <https://doi.org/10.1093/cercor/bhv024>
- Riedel, M. C., Ray, K. L., Dick, A. S., Sutherland, M. T., Hernandez, Z., Fox, P. M., Eickhoff, S. B., Fox, P. T., & Laird, A. R. (2015). Meta-analytic connectivity and behavioral parcellation of the human cerebellum. *NeuroImage*, *117*, 327–342. <https://doi.org/10.1016/j.neuroimage.2015.05.008>
- Riva, D., & Giorgi, C. (2000). The cerebellum contributes to higher functions during development. Evidence from a series of children surgically treated for posterior fossa tumours. *Brain*, *123*(5), 1051–1061. <https://doi.org/10.1093/brain/123.5.1051>
- Robinson, E. C., Jbabdi, S., Glasser, M. F., Andersson, J., Burgess, G. C., Harms, M. P.,

- Smith, S. M., Van Essen, D. C., & Jenkinson, M. (2014). MSM: A new flexible framework for multimodal surface matching. *NeuroImage*, *100*, 414–426.
<https://doi.org/10.1016/j.neuroimage.2014.05.069>
- Ross, L. A., & Olson, I. R. (2010). Social cognition and the anterior temporal lobes. *NeuroImage*, *49*(4), 3452–3462. <https://doi.org/10.1016/j.neuroimage.2009.11.012>
- Salamon, N., Sicotte, N., Drain, A., Frew, A., Alger, J. R., Jen, J., Perlman, S., & Salamon, G. (2007). White matter fiber tractography and color mapping of the normal human cerebellum with diffusion tensor imaging. *Journal of Neuroradiology*, *34*(2), 115–128. <https://doi.org/10.1016/j.neurad.2007.03.002>
- Salmi, J., Pallesen, K. J., Neuvonen, T., Brattico, E., Korvenoja, A., Salonen, O., & Carlson, S. (2010). Cognitive and Motor Loops of the Human Cerebro-cerebellar System. *Journal of Cognitive Neuroscience*, *22*(11), 2663–2676.
<https://doi.org/10.1162/jocn.2009.21382>
- Santiesteban, I., Banissy, M. J., Catmur, C., & Bird, G. (2015). Functional lateralization of temporoparietal junction - imitation inhibition, visual perspective-taking and theory of mind. *European Journal of Neuroscience*, *42*(8), 2527–2533.
<https://doi.org/10.1111/ejn.13036>
- Saxe, R. (2010). The right temporo-parietal junction: a specific brain region for thinking about thoughts. *Handbook of Theory of Mind*, 1–35. [https://doi.org/10.1016/S1053-8119\(03\)00230-1](https://doi.org/10.1016/S1053-8119(03)00230-1)
- Saxe, R., & Wexler, A. (2005). Making sense of another mind: The role of the right temporo-parietal junction. *Neuropsychologia*, *43*(10), 1391–1399.
<https://doi.org/10.1016/j.neuropsychologia.2005.02.013>

- Schilbach, L., Timmermans, B., Reddy, V., Costall, A., Bente, G., Schlicht, T., & Vogeley, K. (2013). Toward a second-person neuroscience. *Behavioral and Brain Sciences*, *36*(4), 393–414. <https://doi.org/10.1017/S0140525X12000660>
- Schiller, D., Freeman, J. B., Mitchell, J. P., Uleman, J. S., & Phelps, E. A. (2009). A neural mechanism of first impressions. *Nature Neuroscience*, *12*(4), 508–514. <https://doi.org/10.1038/nn.2278>
- Schmahmann, J. D. (1991). An Emerging Concept: The Cerebellar Contribution to Higher Function. *Archives of Neurology*, *48*(11), 1178–1187. <https://doi.org/10.1001/archneur.1991.00530230086029>
- Schmahmann, J. D. (1998). Dysmetria of thought: clinical consequences of cerebellar dysfunction on cognition and affect. *Trends in Cognitive Sciences*, *2*(9), 362–371. <https://doi.org/10.1126/science.275.5308.1940>
- Schmahmann, J. D. (2000). The role of the cerebellum in affect and psychosis. *Journal of Neurolinguistics*, *13*(2–3), 189–214. [https://doi.org/10.1016/S0911-6044\(00\)00011-7](https://doi.org/10.1016/S0911-6044(00)00011-7)
- Schmahmann, J. D. (2001). The cerebrocerebellar system: Anatomic substrates of the cerebellar contribution to cognition and emotion. In *International Review of Psychiatry* (Vol. 13, Issue 4, pp. 247–260). Carfax Publishing Company. <https://doi.org/10.1080/09540260120082092>
- Schmahmann, J. D. (2004). Disorders of the cerebellum: Ataxia, dysmetria of thought, and the cerebellar cognitive affective syndrome. In *Journal of Neuropsychiatry and Clinical Neurosciences* (Vol. 16, Issue 3, pp. 367–378). American Psychiatric Publishing Inc. <https://doi.org/10.1176/jnp.16.3.367>

- Schmahmann, J. D. (2019). The cerebellum and cognition. *Neuroscience Letters*, 688(April 2018), 62–75. <https://doi.org/10.1016/j.neulet.2018.07.005>
- Schmahmann, J. D., & Pandya, D. N. (1989). Anatomical investigation of projections to the basis pontis from posterior parietal association cortices in rhesus monkey. *Journal of Comparative Neurology*, 289(1), 53–73. <https://doi.org/10.1002/cne.902890105>
- Schmahmann, J. D., & Pandya, D. N. (1997). The Cerebrocerebellar System. *Int Rev Neurobiol*, 41, 31–60. [https://doi.org/http://dx.doi.org/10.1016/S0074-7742\(08\)60346-3](https://doi.org/http://dx.doi.org/10.1016/S0074-7742(08)60346-3)
- Schmahmann, J. D., & Sherman, J. C. (1998). The cerebellar cognitive affective syndrome. *Brain*, 121(4), 561–579. <https://doi.org/10.1093/brain/121.4.561>
- Schniepp, R., Möhwald, K., & Wuehr, M. (2017). Gait ataxia in humans: vestibular and cerebellar control of dynamic stability. *Journal of Neurology*, 264(1), 87–92. <https://doi.org/10.1007/s00415-017-8482-3>
- Schurz, M., & Perner, J. (2015). An evaluation of neurocognitive models of theory of mind. *Frontiers in Psychology*, 6(OCT), 1–9. <https://doi.org/10.3389/fpsyg.2015.01610>
- Schurz, M., Radua, J., Aichhorn, M., Richlan, F., & Perner, J. (2014). Fractionating theory of mind: A meta-analysis of functional brain imaging studies. *Neuroscience and Biobehavioral Reviews*, 42, 9–34. <https://doi.org/10.1016/j.neubiorev.2014.01.009>
- Scott, R. B., Stoodley, C. J., Anslow, P., Paul, C., Stein, J. F., Sugden, E. M., & Mitchell, C. D. (2007). Lateralized cognitive deficits in children following cerebellar lesions.

Developmental Medicine & Child Neurology, 43(10), 685–691.

<https://doi.org/10.1111/j.1469-8749.2001.tb00142.x>

Segarra, N., Bernardo, M., Valdes, M., Caldu, X., Falcón, C., Rami, L., Bargallo, N., Parramon, G., & Junque, C. (2008). Cerebellar deficits in schizophrenia are associated with executive dysfunction. *NeuroReport*, 19(15), 1513–1517.

<https://doi.org/10.1097/WNR.0b013e3283108bd8>

Shah, S. A., Doraiswamy, P. M., Husain, M. M., Escalona, P. R., Na, C., Figiel, G. S., Patterson, L. J., Ellinwood, E. H., McDonald, W. M., Boyko, O. B., Nemeroff, C. B., & Krishnan, K. R. R. (1992). Posterior fossa abnormalities in major depression: a controlled magnetic resonance imaging study. *Acta Psychiatrica Scandinavica*, 85(6), 474–479. <https://doi.org/10.1111/j.1600-0447.1992.tb03214.x>

Sharma, T., Lancaster, E., Lee, D., Lewis, S., Sigmundsson, T., Takei, N., Gurling, H., Barta, P., Pearlson, G., & Murray, R. (1998). Brain changes in schizophrenia. Volumetric MRI study of families multiply affected with schizophrenia - The Maudsley Family Study 5. In *British Journal of Psychiatry* (Vol. 173, Issue AUG.). <https://doi.org/10.1192/bjp.173.2.132>

Silveri, M. C., Di Betta, A. M., Filippini, V., Leggio, M. G., & Molinari, M. (1998). Verbal short-term store-rehearsal system and the cerebellum. Evidence from a patient with a right cerebellar lesion. *Brain*, 121(11), 2175–2187.

<https://doi.org/10.1093/brain/121.11.2175>

Smith, R., Keramatian, K., & Christoff, K. (2007). Localizing the rostrolateral prefrontal cortex at the individual level. *NeuroImage*, 36(4), 1387–1396.

<https://doi.org/10.1016/j.neuroimage.2007.04.032>

- Smith, S. M., Vidaurre, D., Beckmann, C. F., Glasser, M. F., Jenkinson, M., Miller, K. L., Nichols, T. E., Robinson, E. C., Salimi-Khorshidi, G., Woolrich, M. W., Barch, D. M., Uğurbil, K., & Van Essen, D. C. (2013). Functional connectomics from resting-state fMRI. *Trends in Cognitive Sciences*, *17*(12), 666–682.
<https://doi.org/10.1016/j.tics.2013.09.016>
- Smith, D. V., Gseir, M., Speer, M. E., & Delgado, M. R. (2016). Toward a cumulative science of functional integration: A meta-analysis of psychophysiological interactions. *Human Brain Mapping*, *37*(8), 2904–2917.
<https://doi.org/10.1002/hbm.23216>
- Snider, R. S., Maiti, A., & Snider, S. R. (1976). Cerebellar pathways to ventral midbrain and nigra. *Experimental Neurology*, *53*(3), 714–728. [https://doi.org/10.1016/0014-4886\(76\)90150-3](https://doi.org/10.1016/0014-4886(76)90150-3)
- Sokolov, A. A., Erb, M., Grodd, W., & Pavlova, M. A. (2014). Structural loop between the cerebellum and the superior temporal sulcus: Evidence from diffusion tensor imaging. *Cerebral Cortex*, *24*(3), 626–632. <https://doi.org/10.1093/cercor/bhs346>
- Sørensen, T. (1948). A method of establishing groups of equal amplitude in plant sociology based on similarity of species and its application to analyses of the vegetation on Danish commons. *Kongelige Danske Videnskabernes Selskab*, *5*, 1–34.
- Sotiropoulos, S. N., Hernández-Fernández, M., Vu, A. T., Andersson, J. L., Moeller, S., Yacoub, E., Lenglet, C., Ugurbil, K., Behrens, T. E. J., & Jbabdi, S. (2016). Fusion in diffusion MRI for improved fibre orientation estimation: An application to the 3T and 7T data of the Human Connectome Project. *NeuroImage*, *134*, 396–409.

<https://doi.org/10.1016/j.neuroimage.2016.04.014>

Stephan, K. E., & Friston, K. J. (2010). Analyzing effective connectivity with fMRI.

Wiley Interdisciplinary Reviews: Cognitive Science, 1(3), 446–459.

<https://doi.org/10.1002/wcs.58>

Tavano, A., Grasso, R., Gagliardi, C., Triulzi, F., Bresolin, N., Fabbro, F., & Borgatti, R.

(2007). Disorders of cognitive and affective development in cerebellar

malformations. *Brain*, 130(10), 2646–2660. <https://doi.org/10.1093/brain/awm201>

Thomas, C., Ye, F. Q., Irfanoglu, M. O., Modi, P., Saleem, K. S., Leopold, D. A., &

Pierpaoli, C. (2014). Anatomical accuracy of brain connections derived from

diffusion MRI tractography is inherently limited. *Proceedings of the National*

Academy of Sciences of the United States of America, 111(46), 16574–16579.

<https://doi.org/10.1073/pnas.1405672111>

Tompson, S. H., Kahn, A. E., Falk, E. B., Vettel, J. M., & Bassett, D. S. (2020).

Functional brain network architecture supporting the learning of social networks in

humans. *NeuroImage*, 210, 116498.

<https://doi.org/10.1016/j.neuroimage.2019.116498>

Turchi, J., Chang, C., Ye, F. Q., Russ, B. E., Yu, D. K., Cortes, C. R., Monosov, I. E.,

Duyn, J. H., & Leopold, D. A. (2018). The Basal Forebrain Regulates Global

Resting-State fMRI Fluctuations. *Neuron*, 97(4), 940-952.e4.

<https://doi.org/10.1016/j.neuron.2018.01.032>

Uddin, L. Q., Iacoboni, M., Lange, C., & Keenan, J. P. (2007). The self and social

cognition: the role of cortical midline structures and mirror neurons. *Trends in*

Cognitive Sciences, 11(4), 153–157. <https://doi.org/10.1016/j.tics.2007.01.001>

- Uddin, L. Q., Mooshagian, E., Zaidel, E., Scheres, A., Margulies, D. S., Kelly, A. M. C., Shehzad, Z., Adelstein, J. S., Castellanos, F. X., Biswal, B. B., & Milham, M. P. (2008). Residual functional connectivity in the split-brain revealed with resting-state functional MRI. *NeuroReport*, *19*(7), 703–709.
<https://doi.org/10.1097/WNR.0b013e3282fb8203>
- Van Essen, D. C., Smith, S. M., Barch, D. M., Behrens, T. E. J., Yacoub, E., & Ugurbil, K. (2013). The WU-Minn Human Connectome Project: An overview. *NeuroImage*, *80*, 62–79. <https://doi.org/10.1016/j.neuroimage.2013.05.041>
- Van Essen, D. C., Ugurbil, K., Auerbach, E., Barch, D., Behrens, T. E. J., Bucholz, R., Chang, A., Chen, L., Corbetta, M., Curtiss, S. W., Della Penna, S., Feinberg, D., Glasser, M. F., Harel, N., Heath, A. C., Larson-Prior, L., Marcus, D., Michalareas, G., Moeller, S., ... Yacoub, E. (2012). The Human Connectome Project: A data acquisition perspective. *NeuroImage*, *62*(4), 2222–2231.
<https://doi.org/10.1016/j.neuroimage.2012.02.018>
- Van Overwalle, F. (2009). Social cognition and the brain: A meta-analysis. In *Human Brain Mapping* (Vol. 30, Issue 3, pp. 829–858). Wiley-Blackwell.
<https://doi.org/10.1002/hbm.20547>
- Van Overwalle, F., & Baetens, K. (2009). Understanding others' actions and goals by mirror and mentalizing systems: A meta-analysis. *NeuroImage*, *48*(3), 564–584.
<https://doi.org/10.1016/J.NEUROIMAGE.2009.06.009>
- Van Overwalle, F., Baetens, K., Mariën, P., & Vandekerckhove, M. (2014). Social cognition and the cerebellum: A meta-analysis of over 350 fMRI studies. In *NeuroImage* (Vol. 86, pp. 554–572). Academic Press.

<https://doi.org/10.1016/j.neuroimage.2013.09.033>

Van Overwalle, F., Baetens, K., Mariën, P., & Vandekerckhove, M. (2015). Cerebellar areas dedicated to social cognition? A comparison of meta-analytic and connectivity results. *Social Neuroscience, 10*(4), 337–344.

<https://doi.org/10.1080/17470919.2015.1005666>

Van Overwalle, F., D’aes, T., & Mariën, P. (2015). Social cognition and the cerebellum: A meta-analytic connectivity analysis. *Human Brain Mapping, 36*(12), 5137–5154.

<https://doi.org/10.1002/hbm.23002>

Van Overwalle, F., & Mariën, P. (2016). Functional connectivity between the cerebrum and cerebellum in social cognition: A multi-study analysis. *NeuroImage, 124*, 248–255. <https://doi.org/10.1016/j.neuroimage.2015.09.001>

Van Overwalle, F., & Vandekerckhove, M. (2013). Implicit and explicit social mentalizing: dual processes driven by a shared neural network. *Frontiers in Human Neuroscience, 7*(SEP), 560. <https://doi.org/10.3389/fnhum.2013.00560>

Varnäs, K., Okugawa, G., Hammarberg, A., Nesvåg, R., Rimol, L. M., Franck, J., & Agartz, I. (2007). Cerebellar volumes in men with schizophrenia and alcohol dependence. *Psychiatry and Clinical Neurosciences, 61*(3), 326–329.

<https://doi.org/10.1111/j.1440-1819.2007.01661.x>

Voogd, J., & Glickstein, M. (1998). The anatomy of the cerebellum. In *Trends in Cognitive Sciences* (Vol. 2, Issue 9, pp. 307–313). Elsevier Current Trends.

[https://doi.org/10.1016/S1364-6613\(98\)01210-8](https://doi.org/10.1016/S1364-6613(98)01210-8)

Wakana, S., Caprihan, A., Panzenboeck, M. M., Fallon, J. H., Perry, M., Gollub, R. L., Hua, K., Zhang, J., Jiang, H., Dubey, P., Blitz, A., van Zijl, P., & Mori, S. (2007).

- Reproducibility of quantitative tractography methods applied to cerebral white matter. *NeuroImage*, 36(3), 630–644.
<https://doi.org/10.1016/j.neuroimage.2007.02.049>
- Wang, Y., Collins, J. A., Koski, J., Nugiel, T., Metoki, A., & Olson, I. R. (2017). Dynamic neural architecture for social knowledge retrieval. *Proceedings of the National Academy of Sciences*, 114(16), E3305–E3314.
<https://doi.org/10.1073/pnas.1621234114>
- Wang, Y., Metoki, A., Xia, Y., Zang, Y., He, Y., Olson, I. R. (2020). *A Large-Scale Structural and Functional Connectome of Social Mentalizing*. [Manuscript submitted for publication]. Department of Psychology, Temple University
- Watson, T. C., Obiang, P., Torres-Herraez, A., Watilliaux, A., Coulon, P., Rochefort, C., & Rondi-Reig, L. (2019). Anatomical and physiological foundations of cerebello-hippocampal interaction. *ELife*, 8. <https://doi.org/10.7554/eLife.41896.001>
- Wheatley, T., Milleville, S. C., & Martin, A. (2007). Understanding animate agents: Distinct roles for the social network and mirror system: Research report. *Psychological Science*, 18(6), 469–474. <https://doi.org/10.1111/j.1467-9280.2007.01923.x>
- White, S. J., Coniston, D., Rogers, R., & Frith, U. (2011). Developing the Frith-Happé animations: A quick and objective test of Theory of Mind for adults with autism. *Autism Research*, 4(2), 149–154. <https://doi.org/10.1002/aur.174>
- Whitney, E. R., Kemper, T. L., Bauman, M. L., Rosene, D. L., & Blatt, G. J. (2008). Cerebellar Purkinje cells are reduced in a subpopulation of autistic brains: A stereological experiment using calbindin-D28k. *Cerebellum*, 7(3), 406–416.

<https://doi.org/10.1007/s12311-008-0043-y>

WU - Minn Consortium Human Connectome Projec. (2015). *Reference Manual – 900*

Subjects Release. December. <http://www.cmrr.umn.edu/multiband/>

Yang, D. Y. J., Rosenblau, G., Keifer, C., & Pelphrey, K. A. (2015). An integrative neural model of social perception, action observation, and theory of mind.

Neuroscience and Biobehavioral Reviews, *51*, 263–275.

<https://doi.org/10.1016/j.neubiorev.2015.01.020>

Yeo, B. T. T., Krienen, F. M., Sepulcre, J., Sabuncu, M. R., Lashkari, D., Hollinshead, M., Roffman, J. L., Smoller, J. W., Zöllei, L., Polimeni, J. R., Fisch, B., Liu, H., & Buckner, R. L. (2011). The organization of the human cerebral cortex estimated by intrinsic functional connectivity. *Journal of Neurophysiology*, *106*(3), 1125–1165.

<https://doi.org/10.1152/jn.00338.2011>

Zanchetti, A., & Zoccolini, A. (1954). Autonomic hypothalamic outbursts elicited by cerebellar stimulation. *Journal of Neurophysiology*, *17*(5), 475–483.

Zeidman, P., Jafarian, A., Corbin, N., Seghier, M. L., Razi, A., Price, C. J., & Friston, K. J. (2019). A guide to group effective connectivity analysis, part 1: First level analysis with DCM for fMRI. *NeuroImage*, *200*, 174–190.

<https://doi.org/10.1016/j.neuroimage.2019.06.031>

APPENDIX

SUPPLEMENTARY TABLES

Table A1. Cerebellar clusters of activation and cerebellar lobule percentage overlap.
Percentages > 10% are in bold.

Cerebellar lobes	Cerebellar lobules	Emotion	Language	Motor	Relational Memory	ToM	Working Memory
Left anterior lobe	Left I-IV	0.00		1.60			0.00
	Left V			5.34		0.00	0.02
Left superior posterior lobe	Left VI	9.95		19.90	5.74	5.14	8.88
	Left Crus I	5.14	7.70	4.95	21.97	13.82	22.68
	Left Crus II	25.41	9.61	0.09	30.41	20.40	12.61
	Left VIIb	7.85	0.01	2.95	7.00	7.68	5.33
Left inferior posterior lobe	Left VIIIa	0.19		4.08	0.00	1.10	0.44
	Left VIIIb	0.30	0.01	0.02		0.11	0.18
	Left IX	0.39	1.41			4.34	0.75
Left flocculonodular lobe	Left X	4.77				1.05	0.01
Right anterior lobe	Right I-IV			3.32			
	Right V	0.00		6.79		0.00	0.01
Right superior posterior lobe	Right VI	3.09	1.13	20.93	4.66	3.86	7.71
	Right Crus I	1.58	29.03	6.18	24.71	11.04	17.61
	Right Crus II	6.68	40.12	0.33	1.49	16.49	7.33
	Right VIIb	1.40	0.19	4.27		2.97	6.36
Right inferior posterior lobe	Right VIIIa	0.09		7.26		0.04	1.25
	Right VIIIb	0.27	0.01	0.38		0.06	0.01
	Right IX	0.20	3.63	0.01		0.91	
Right flocculonodular lobe	Right X	4.30	0.01	0.00		0.86	0.01
Vermis	Vermis VI	10.86		1.93	0.03		0.57
	Vermis Crus I	1.09		0.00	0.06		0.10
	Vermis Crus II	3.65			0.03		0.07
	Vermis VIIb	0.18		0.00			0.00
	Vermis VIIIa	0.05		0.03		0.01	
	Vermis VIIIb	0.03	0.04	0.01		0.10	
	Vermis IX	2.04	0.31			2.36	
	Vermis X	0.65	0.03			0.51	

Table A2. One-sample Kolmogorov-Smirnov test for normality distribution of beta weights (effective connectivity) of all tasks. Significant results are in bold.

	One-sample Kolmogorov-Smirnov test		
	D value	df	Sig.
emotion	.06	671	.00
language	.06	671	.00
motor	.05	671	.00
relational	.08	671	.00
ToM	.07	671	.00
wm	.07	671	.00

Table A3. Spearman's rho correlations between task activations. Significant results are in bold.

	emotion	language	motor	relational	ToM	wm
emotion						
language	.12**					
motor	-.01	-.05				
relational	.10**	.07	.07			
ToM	.01	.14**	.05	.07		
wm	.05	.05	.15**	.22**	.18**	

**Correlation is significant at the 0.01 level (two-tailed).

Table A4. Wilcoxon signed-rank test results for all possible task pairs. Significant results are in bold.

	Negative ranks			Positive ranks			Test statistics		
	<i>n</i>	Mean Rank	Sum of Ranks	<i>n</i>	Mean Rank	Sum of Ranks	Ties	<i>Z</i>	<i>p</i>
(language)–(emotion)	272	317.63	86394	399	348.53	139062	0	-5.24^b	.00*
(motor)–(emotion)	83	16.72	13340	588	36.74	212116	0	-19.79^b	.00*
(relational)–(emotion)	345	321.00	110745	326	351.87	114711	0	-.40 ^b	.69
(ToM)–(emotion)	219	276.57	60569	452	364.79	164887	0	-1.38^b	.00*
(wm)–(emotion)	67	114.73	7687	604	36.54	217769	0	-2.91^b	.00*
(motor)–(language)	115	191.50	22022	556	365.89	203434	0	-18.06^b	.00*
(relational)–(language)	381	342.47	130482.50	290	327.49	94973.50	0	-3.54^a	.00*
(ToM)–(language)	264	297.78	78613	407	36.79	146843	0	-6.79^a	.00*
(wm)–(language)	82	15.80	12366	589	361.78	213090	0	-19.98^a	.00*
(relational)–(motor)	577	359.66	207521	94	19.80	17935	0	-18.87^b	.00*
(ToM)–(motor)	513	373.46	191586	158	214.37	33870	0	-15.70^b	.00*
(wm)–(motor)	250	294.76	73691	421	36.49	151765	0	-7.77^a	.00*
(ToM)–(relational)	222	308.44	68474	449	349.63	156982	0	-8.81^a	.00*
(wm)–(relational)	69	11.12	7598	602	361.89	217858	0	-2.93^a	.00*
(wm)–(ToM)	104	168.42	17516	567	366.74	207940	0	-18.96^a	.00*

*Indicates statistically significant change

^aBased on negative ranks

^bBased on positive ranks

Table A5. Paired samples t-tests on individual beta-weights (effective connectivity) for all proximal ROIs. Significant results are in bold.

	Mean	Std Dev	Paired <i>t</i> test		
			<i>t</i> value	df	Sig. (two-tailed)
<i>L5 – L5a</i>					
L5_R_ATL	.02	.49	-1.18	670	.24
L5a_R_ATL	.04	.46			
L5_R_DMPFC	-.05	.50	.44	670	.66
L5a_R_DMPFC	-.06	.51			
L5_R_PreC	.08	.51	-1.65	670	.10
L5a_R_PreC	.12	.57			
L5_R_TPJ	.07	.55	1.64	670	.10
L5a_R_TPJ	.03	.55			
L5_R_VMPFC	.04	.45	-.44	670	.66
L5a_R_VMPFC	.05	.47			
<i>L6 – L6a</i>					
L6_R_ATL	.07	.47	.89	670	.38
L6a_R_ATL	.05	.47			
L6_R_DMPFC	.03	.46	-1.08	670	.28
L6a_R_DMPFC	.06	.47			
L6_R_PreC	.08	.51	5.72	670	.00
L6a_R_PreC	-.04	.49			
L6_R_VMPFC	.01	.47	-4.23	670	.00
L6a_R_VMPFC	.10	.49			
<i>L7 – L7a</i>					
L7_R_ATL	.09	.49	4.81	670	.00
L7a_R_ATL	-.01	.55			
L7_R_DMPFC	.08	.51	1.71	670	.09
L7a_R_DMPFC	.05	.50			
L7_R_PreC	.03	.53	7.31	670	.00
L7a_R_PreC	-.11	.56			
L7_R_TPJ	.10	.57	8.81	670	.00
L7a_R_TPJ	-.07	.54			
L7_R_VMPFC	.18	.54	4.77	670	.00
L7a_R_VMPFC	.09	.49			
<i>R1 – R1a</i>					
R1_L_ATL	.07	.46	-.72	670	.47
R1a_L_ATL	.09	.51			
R1_L_DMPFC	.02	.50	-1.13	670	.26
R1a_L_DMPFC	.05	.47			
R1_L_TPJ	.09	.51	-1.14	670	.26

R1a_L_TPJ	.11	.52			
R1_L_VMPFC	.06	.48	1.08	670	.28
R1a_L_VMPFC	.04	.47			

Table A6. Wilcoxon signed ranks test on individual beta-weights (effective connectivity) for proximal ROIs not meeting normality criteria. Significant results are in bold.

	Wilcoxon signed ranks test	
	Z value	Sig. (two-tailed)
<u>L6 – L6a</u>		
L6_R_TPJ	-1.84	.07
L6a_R_TPJ		
<u>L7 – L7a</u>		
L7_R_TPJ	-8.41	.00
L7a_R_TPJ		
<u>R1 – R1a</u>		
R1_L_PreC	-1	.32
R1a_L_PreC		

Table A7. Cerebello-thalamo-cortical white matter pathways average streamline counts. Results for each cerebellar lobe and the averaged whole CTC and CPC are in bold.

	Streamline count			Streamline count	
	Mean	SD		Mean	SD
Left CTC	35.52	(13.67)	Right CTC	32.76	(35.73)
Left superior posterior lobe	24.27	(26.93)	Right superior posterior lobe	32.26	(35.79)
L1-R_ATL	7.26	(13.67)	R1-L_ATL	8.75	(21.19)
L1-R_DMPFC	80.17	(84.47)	R1-L_DMPFC	100.40	(98.79)
L1-R_PreC	21.18	(36.19)	R1-L_PreC	29.22	(38.89)
L1-R_TPJ	4.65	(10.62)	R1-L_TPJ	4.85	(9.99)
L1-R_VMPFC	33.47	(47.37)	R1-L_VMPFC	38.30	(66.03)
			R1a-L_ATL	8.86	(21.61)
			R1a-L_DMPFC	98.88	(94.63)
			R1a-L_PreC	29.43	(39.13)
			R1a-L_TPJ	4.52	(9.72)
			R1a-L_VMPFC	39.21	(68.69)
L2-R_ATL	9.62	(17.18)	R2-L_ATL	11.65	(21.67)
L2-R_DMPFC	112.91	(128.06)	R2-L_DMPFC	143.06	(160.77)
L2-R_PreC	28.25	(40.34)	R2-L_PreC	41.97	(51.97)
L2-R_TPJ	7.22	(20.47)	R2-L_TPJ	6.96	(13.21)
L2-R_VMPFC	48.28	(77.53)	R2-L_VMPFC	54.87	(90.42)
L3-R_ATL	4.01	(8.18)	R3-L_ATL	3.62	(8.80)
L3-R_DMPFC	48.55	(65.79)	R3-L_DMPFC	42.08	(50.82)
L3-R_PreC	12.39	(22.01)	R3-L_PreC	13.06	(17.96)
L3-R_TPJ	2.73	(6.27)	R3-L_TPJ	2.03	(4.71)
L3-R_VMPFC	21.2	(45.41)	R3-L_VMPFC	16.25	(26.35)
L4-R_ATL	6.81	(10.49)	R4-L_ATL	5.23	(10.85)
L4-R_DMPFC	78.37	(90.26)	R4-L_DMPFC	58.33	(69.50)
L4-R_PreC	21.13	(41.09)	R4-L_PreC	18.83	(31.59)
L4-R_TPJ	4.82	(12.42)	R4-L_TPJ	2.84	(6.52)
L4-R_VMPFC	33.49	(53.01)	R4-L_VMPFC	23.23	(43.42)
L7-R_ATL	3.23	(6.86)			
L7-R_DMPFC	39.76	(60.18)			
L7-R_PreC	9.66	(16.15)			
L7-R_TPJ	2.25	(5.72)			
L7-R_VMPFC	16.47	(31.70)			
L7a-R_ATL	3.1	(6.40)			
L7a-R_DMPFC	39.03	(56.93)			
L7a-R_PreC	9.92	(18.13)			

L7a-R_TPJ	2.24	(5.78)		
L7a-R_VMPFC	15.87	(30.79)		
Left inferior posterior lobe	38.42	(41.90)	Right inferior posterior lobe	22.04 (22.76)
L5-R_ATL	6.25	(10.14)	R5-L_ATL	5.42 (11.28)
L5-R_DMPFC	71	(80.34)	R5-L_DMPFC	59.57 (70.72)
L5-R_PreC	19.27	(29.65)	R5-L_PreC	17.96 (24.36)
L5-R_TPJ	4.23	(10.39)	R5-L_TPJ	2.91 (6.33)
L5-R_VMPFC	31.01	(52.30)	R5-L_VMPFC	24.34 (44.99)
L5a-R_ATL	11.78	(17.70)		
L5a-R_DMPFC	139.34	(134.45)		
L5a-R_PreC	34.61	(55.27)		
L5a-R_TPJ	9.32	(23.67)		
L5a-R_VMPFC	57.38	(79.88)		
Left flocculonodular lobe	56.10	(58.60)	Right flocculonodular lobe	45.99 (47.81)
L6-R_ATL	11.46	(15.54)	R6-L_ATL	11.31 (22.76)
L6-R_DMPFC	132.81	(125.52)	R6-L_DMPFC	125.54 (110.95)
L6-R_PreC	35.59	(50.65)	R6-L_PreC	39.66 (49.49)
L6-R_TPJ	8.86	(24.91)	R6-L_TPJ	6.37 (10.73)
L6-R_VMPFC	55.38	(68.56)	R6-L_VMPFC	47.10 (58.77)
L6a-R_ATL	10.06	(13.35)		
L6a-R_DMPFC	117.07	(109.76)		
L6a-R_PreC	31.78	(48.23)		
L6a-R_TPJ	8.11	(27.19)		
L6a-R_VMPFC	49.1	(60.73)		
L7-R_ATL	16.99	(25.48)		
L7-R_DMPFC	211.01	(179.70)		
L7-R_PreC	50.41	(59.08)		
L7-R_TPJ	11.72	(27.44)		
L7-R_VMPFC	91.22	(113.75)		

Table A8. Cortico-ponto-cerebellar white matter pathways average streamline counts. Results for each cerebellar lobe and the averaged whole CTC and CPC are in bold.

	Streamline count			Streamline count	
	Mean	SD		Mean	SD
Left CPC	28.04	(33.81)	Right CPC	21.74	(25.30)
Left superior posterior lobe	17.82	(19.26)	Right superior posterior lobe	20.89	(19.93)
R_ATL-L1	15.96	(17.86)	L_ATL-R1	12.99	(15.50)
R_DMPFC-L1	72.64	(98.81)	L_DMPFC-R1	72.82	(87.45)
R_PreC-L1	10.92	(13.11)	L_PreC-R1	19.85	(21.81)
R_TPJ-L1	23.08	(33.07)	L_TPJ-R1	15.34	(29.55)
R_VMPFC-L1	21.38	(42.25)	L_VMPFC-R1	18.76	(38.54)
			L_ATL-R1a	12.32	(13.39)
			L_DMPFC-R1a	67.38	(78.16)
			L_PreC-R1a	18.78	(21.52)
			L_TPJ-R1a	14.73	(26.95)
			L_VMPFC-R1a	18.50	(39.59)
R_ATL-L2	15.81	(17.84)	L_ATL-R2	11.79	(13.64)
R_DMPFC-L2	71.99	(84.57)	L_DMPFC-R2	66.68	(87.66)
R_PreC-L2	13.32	(27.04)	L_PreC-R2	19.02	(24.39)
R_TPJ-L2	23.77	(39.17)	L_TPJ-R2	13.84	(20.04)
R_VMPFC-L2	18.80	(33.76)	L_VMPFC-R2	15.96	(34.09)
R_ATL-L3	5.37	(7.12)	L_ATL-R3	3.42	(5.37)
R_DMPFC-L3	25.25	(40.25)	L_DMPFC-R3	20.73	(30.74)
R_PreC-L3	4.33	(7.97)	L_PreC-R3	5.26	(8.02)
R_TPJ-L3	8.23	(15.01)	L_TPJ-R3	4.21	(9.36)
R_VMPFC-L3	7.06	(26.53)	L_VMPFC-R3	4.02	(9.31)
R_ATL-L4	15.66	(18.74)	L_ATL-R4	7.92	(10.16)
R_DMPFC-L4	66.82	(89.37)	L_DMPFC-R4	45.59	(57.27)
R_PreC-L4	10.35	(13.65)	L_PreC-R4	12.09	(14.93)
R_TPJ-L4	24.00	(35.34)	L_TPJ-R4	9.73	(23.76)
R_VMPFC-L4	17.47	(36.53)	L_VMPFC-R4	10.48	(22.34)
R_ATL-L7	4.26	(6.60)			
R_DMPFC-L7	17.58	(26.19)			
R_PreC-L7	3.16	(5.54)			
R_TPJ-L7	6.36	(11.97)			
R_VMPFC-L7	4.62	(11.40)			
R_ATL-L7a	3.25	(5.17)			
R_DMPFC-L7a	12.98	(19.31)			
R_PreC-L7a	2.30	(4.18)			

R_TPJ-L7a	4.58	(7.69)			
R_VMPFC-L7a	3.38	(10.53)			
Left inferior posterior lobe	13.96	(14.36)	Right inferior posterior lobe	1.86	(1.62)
R_ATL-L5	4.15	(5.85)	L_ATL-R5	0.93	(2.51)
R_DMPFC-L5	17.68	(24.50)	L_DMPFC-R5	4.75	(7.81)
R_PreC-L5	2.82	(4.14)	L_PreC-R5	1.19	(2.18)
R_TPJ-L5	5.89	(8.96)	L_TPJ-R5	1.05	(3.25)
R_VMPFC-L5	6.52	(16.59)	L_VMPFC-R5	1.40	(4.03)
R_ATL-L5a	10.20	(11.47)			
R_DMPFC-L5a	51.66	(68.38)			
R_PreC-L5a	7.57	(9.46)			
R_TPJ-L5a	14.23	(17.50)			
R_VMPFC-L5a	18.91	(33.61)			
Left flocculonodular lobe	57.84	(46.81)	Right flocculonodular lobe	45.87	(42.73)
R_ATL-L6	34.74	(36.06)	L_ATL-R6	21.82	(22.65)
R_DMPFC-L6	138.17	(170.01)	L_DMPFC-R6	121.89	(140.21)
R_PreC-L6	22.50	(26.27)	L_PreC-R6	33.73	(34.68)
R_TPJ-L6	54.44	(72.23)	L_TPJ-R6	27.97	(69.82)
R_VMPFC-L6	33.34	(48.08)	L_VMPFC-R6	23.94	(42.36)
R_ATL-L6a	38.34	(43.20)			
R_DMPFC-L6a	144.61	(164.80)			
R_PreC-L6a	25.14	(30.59)			
R_TPJ-L6a	60.58	(81.73)			
R_VMPFC-L6a	31.18	(44.83)			
R_ATL-L7	22.69	(6.60)			
R_DMPFC-L7	150.01	(26.19)			
R_PreC-L7	20.27	(5.54)			
R_TPJ-L7	27.15	(11.97)			
R_VMPFC-L7	64.50	(11.40)			

Table A9. One-sample Kolmogorov-Smirnov test for normality distribution of cerebello-thalamo-cortical and cortico-ponto-cerebellar white matter pathway streamline counts (cerebellar lobe averages). Significant results are in bold.

		One-sample Kolmogorov-Smirnov test		
		<i>D</i> value	df	Sig.
CTC	Left cerebellum to right cerebrum	0.12	671	.00
	Superior posterior lobe	0.16	671	.00
	Inferior posterior lobe	0.14	671	.00
	Flocculonodular lobe	0.12	671	.00
	Right cerebellum to left cerebrum	0.14	671	.00
	Superior posterior lobe	0.14	671	.00
	Inferior posterior lobe	0.19	671	.00
	Flocculonodular lobe	0.13	671	.00
	Left cerebrum to right cerebellum	0.14	671	.00
	Superior posterior lobe	0.14	671	.00
	Inferior posterior lobe	0.25	671	.00
	Flocculonodular lobe	0.15	671	.00
CPC	Right cerebrum to left cerebellum	0.14	671	.00
	Superior posterior lobe	0.14	671	.00
	Inferior posterior lobe	0.17	671	.00
	Flocculonodular lobe	0.14	671	.00

Table A10. Spearman's rho correlations between cerebello-thalamo-cortical streamline counts averaged across cerebellar lobes. Bold indicates the correlation of interest (e.g. left superior lobe correlated to right superior lobe streamline count). Blue boxes enclose correlations between right-left CTC streamline counts.

		Left cerebellum to right cerebrum			Right cerebellum to left cerebrum		
		Superior or posterior lobe	Inferior posterior lobe	Flocculonodular lobe	Superior or posterior lobe	Inferior posterior lobe	Flocculonodular lobe
Left cerebellum to right cerebrum	Superior posterior lobe	1	.642**	.774**	.230**	.121**	.191**
	Inferior posterior lobe	.642**	1	.845**	.148**	.275**	.179**
	Flocculonodular lobe	.774**	.845**	1	.179**	.162**	.234**
Right cerebellum to left cerebrum	Superior posterior lobe	.230**	.148**	.179**	1	.534**	.697**
	Inferior posterior lobe	.121**	.275**	.162**	.534**	1	.599**
	Flocculonodular lobe	.191**	.179**	.234**	.697**	.599**	1

**Correlation is significant at the 0.01 level (two-tailed).

Table A11. Spearman's rho correlations between cortico-ponto-cerebellar streamline counts averaged across cerebellar lobes. Bold indicates the correlation of interest (eg. left superior lobe correlated to right superior lobe streamline count). Blue boxes enclose correlations between right-left CPC streamline counts.

		Left cerebrum to right cerebellum			Right cerebrum to left cerebellum		
		Superior or posterior lobe	Inferior posterior lobe	Flocculonodular lobe	Superior or posterior lobe	Inferior posterior lobe	Flocculonodular lobe
Left cerebrum to right cerebellum	Superior posterior lobe	1	.557**	.825**	.240**	.201**	.204**
	Inferior posterior lobe	.557**	1	.641**	.106**	.251**	.160**
	Flocculonodular lobe	.825**	.641**	1	.164**	.207**	.215**
Right cerebrum to left cerebellum	Superior posterior lobe	.240**	.106**	.164**	1	.688**	.860**
	Inferior posterior lobe	.201**	.251**	.207**	.688**	1	.829**
	Flocculonodular lobe	.204**	.160**	.215**	.860**	.829**	1

**Correlation is significant at the 0.01 level (two-tailed).

Table A12. Wilcoxon signed-rank test results for all possible left-right streamline count cerebellar hemisphere and lobe pairs. Significant results are in bold.

	Negative ranks			Positive ranks			Test statistics		
	<i>n</i>	Mean Rank	Sum of Ranks	<i>n</i>	Mean Rank	Sum of Ranks	Ties	<i>Z</i>	<i>p</i>
CTC R – CTC L	372	340.75	126759.50	297	327.80	97355.50	2	-2.94^b	.003*
(SPR)–(SPL)	235	297.57	69930	433	354.54	153516	3	-8.38^a	.00*
(IPR)–(IPL)	503	359.68	180919	166	260.22	43196	2	-13.77^b	.00*
(FR)–(FL)	429	341.68	146581	240	323.06	77534	2	-6.90^b	.00*
CPC R – CPC L	424	349.52	148197.50	245	309.87	75917.50	2	-7.23^b	.00*
(SPR)–(SPL)	300	311.49	93446	369	354.12	130669	2	-3.72^a	.00*
(IPR)–(IPL)	649	339.66	220437.50	18	130.03	2340.50	4	-21.91^b	.00*
(FR)–(FL)	404	355.75	143724.50	265	303.36	80390.50	2	-6.33^b	.00*
CPC R – CTC R	484	357.61	173081.50	184	273.72	50364.5	3	-12.30^b	.00*
CPC L – CTC L	434	353.97	153.624	235	299.96	70491	2	-8.31^b	.00*

*Indicates statistically significant change

^aBased on negative ranks

^bBased on positive ranks

CTC: cerebello-thalamo-cortical pathway, CPC: cortico-ponto-cerebellar pathway, SPR: superior posterior right lobe, SPL: superior posterior left lobe, IPR: inferior posterior right lobe, IPL: inferior posterior left lobe, FR: flocculonodular right lobe, FL: flocculonodular left lobe